

NASA/CR-2015-218679



Elemental Water Impact Test: Phase 1 20-inch Hemisphere

Gregory J. Vassilakos
Analytical Mechanics Associates, Inc., Hampton, Virginia

January 2015

NASA STI Program . . . in Profile

Since its founding, NASA has been dedicated to the advancement of aeronautics and space science. The NASA scientific and technical information (STI) program plays a key part in helping NASA maintain this important role.

The NASA STI program operates under the auspices of the Agency Chief Information Officer. It collects, organizes, provides for archiving, and disseminates NASA's STI. The NASA STI program provides access to the NTRS Registered and its public interface, the NASA Technical Reports Server, thus providing one of the largest collections of aeronautical and space science STI in the world. Results are published in both non-NASA channels and by NASA in the NASA STI Report Series, which includes the following report types:

- **TECHNICAL PUBLICATION.** Reports of completed research or a major significant phase of research that present the results of NASA Programs and include extensive data or theoretical analysis. Includes compilations of significant scientific and technical data and information deemed to be of continuing reference value. NASA counter-part of peer-reviewed formal professional papers but has less stringent limitations on manuscript length and extent of graphic presentations.
- **TECHNICAL MEMORANDUM.** Scientific and technical findings that are preliminary or of specialized interest, e.g., quick release reports, working papers, and bibliographies that contain minimal annotation. Does not contain extensive analysis.
- **CONTRACTOR REPORT.** Scientific and technical findings by NASA-sponsored contractors and grantees.

- **CONFERENCE PUBLICATION.** Collected papers from scientific and technical conferences, symposia, seminars, or other meetings sponsored or co-sponsored by NASA.
- **SPECIAL PUBLICATION.** Scientific, technical, or historical information from NASA programs, projects, and missions, often concerned with subjects having substantial public interest.
- **TECHNICAL TRANSLATION.** English-language translations of foreign scientific and technical material pertinent to NASA's mission.

Specialized services also include organizing and publishing research results, distributing specialized research announcements and feeds, providing information desk and personal search support, and enabling data exchange services.

For more information about the NASA STI program, see the following:

- Access the NASA STI program home page at <http://www.sti.nasa.gov>
- E-mail your question to help@sti.nasa.gov
- Phone the NASA STI Information Desk at 757-864-9658
- Write to:
NASA STI Information Desk
Mail Stop 148
NASA Langley Research Center
Hampton, VA 23681-2199

NASA/CR-2014-218679



Elemental Water Impact Test: Phase 1 20-Inch Hemisphere

Gregory J. Vassilakos
Analytical Mechanics Associates, Inc., Hampton, Virginia

National Aeronautics and
Space Administration

Langley Research Center
Hampton, Virginia 23681-2199

Prepared for Langley Research Center
under Contract NNL12AA09C

January 2015

Acknowledgments

The author would like to recognize Dr. Karen Lyle, Steve Gayle, and Dr. Peter Gage for developing the plan for the test series and arranging the set-up of the test facility and fabrication of the test article. The author would like to thank David Stegall for his exhaustive efforts in providing test data and troubleshooting problems with the instrumentation and data acquisition system. The author would also like to thank Mercedes Reaves for the investigations into coupling stiffness and gravitational preload that she performed using 3-D models of the hemisphere. The author would also like to recognize Claude Bryant for bringing attention to the Cappelli and Wilkinson equations and for his efforts in troubleshooting problems with the 2-D axisymmetric model.

The use of trademarks or names of manufacturers in this report is for accurate reporting and does not constitute an official endorsement, either expressed or implied, of such products or manufacturers by the National Aeronautics and Space Administration.

Available from:

NASA STI Program / Mail Stop 148
NASA Langley Research Center
Hampton, VA 23681-2199
Fax: 757-864-6500

THIS PAGE INTENTIONALLY LEFT BLANK

Abstract

Spacecraft are being designed based on LS-DYNA simulations of water landing impacts. The Elemental Water Impact Test (EWIT) series was undertaken to assess the accuracy of LS-DYNA water impact simulations. Phase 1 of the EWIT series featured water impact tests of a 20-inch hemisphere dropped from heights of 5 feet and 10 feet. The hemisphere was outfitted with an accelerometer and three pressure gages. The focus of this report is the correlation of analytical models against test data. Three analytical models were used:

1. Closed-Form Solution
2. 2-D Axisymmetric LS-DYNA Model
3. 3-D Quarter Symmetry LS-DYNA Model

The closed form solution was found to over-predict the peak acceleration. The peak pressure from the closed-form solution is infinite; however, the solution does provide a reasonable prediction for the late-time pressure decay.

The 2-D axisymmetric LS-DYNA model was evaluated for a broad range of modeling parameters. The two parameters that were found to be the most critical were mesh density and fluid-structure coupling stiffness. The 2-D model provided reasonable predictions for the acceleration histories. Pressure histories were poorly predicted; however, reasonable predictions were obtained for the impulse as determined by integrating the pressure history. Increasing mesh density resulted in better predictions for the late-time pressure decay, but did not improve the predictions of the early-time peak pressure.

The 3-D quarter symmetry LS-DYNA model was used for further evaluations of mesh density and fluid structure coupling stiffness. The 3-D model produced predictions for the acceleration histories that better matched the test data than the 2-D model. The pressure histories from the 3-D model were equally as poor as the 2-D model. Again, the impulse was predicted far more accurately than the pressure.

The following guidelines were proposed for defining the fluid mesh density and fluid-structure coupling stiffness for LS-DYNA simulations. These guidelines might not be feasible for spacecraft water landing design simulations due to limits in available computer resources.

1. The element size of the fluid mesh should be no larger than 1/200th of the radius of curvature of the structure.
2. The coupling stiffness curve should be established based on the maximum expected coupling pressure at a penetration equal to 1/10th the size of the fluid elements.

Guidelines were also offered for judging the adequacy of the fluid-structure coupling definition.

1. The coupling stiffness is too soft if the peak coupling pressure is toward the middle of the contact patch rather than at the perimeter.
2. The coupling stiffness is too soft if the acceleration time history exhibits oscillations that can be related to the structure bouncing on the coupling surface.
3. The coupling stiffness is too stiff if the coupling pressure distribution appears as a checkerboard pattern of isolated pressure spikes.
4. The coupling stiffness is too stiff if the coupling pressure histories appear as a series of isolated spikes.

Table of Contents

1. Introduction	1
2. Simulations	1
2.1. LS-DYNA	1
2.2. ALE Solution Parameters	1
2.3. Element Section Parameters	2
2.4. Material Parameters	2
2.5. Equation of State Parameters	2
2.6. Fluid Structure Coupling Parameters	2
2.7. Boundary Conditions	2
2.8. Gravity and Atmospheric Preload	3
3. Tests	3
3.1. Test Configuration	3
3.2. Test Article	4
3.3. Test Results	5
4. Simulation Models	8
4.1. Closed-Form Solution	8
4.2. 2-D LS-DYNA Simulation	9
4.3. 3-D LS-DYNA Simulation	11
5. Test and Simulation Correlation	13
5.1. Closed-Form Results	13
5.2. 2-D LS-DYNA Results	15
5.3. 3-D LS-DYNA Results	30
6. Establishing Simulation Parameters without Test Data	38
6.1. Width of Pressure Pulse	38
6.2. Establishing Mesh Density and Coupling Stiffness	39
6.3. Evaluating Model Performance without Test Data	40
7. Conclusions and Recommendations	43
References	44
Appendix A: Two-Dimensional Axisymmetric Model	45
Appendix B: Three-Dimensional Quarter Model	48

List of Figures

Figure 1. Test Set-Up.....	4
Figure 2. Hemisphere Configuration	4
Figure 3. Pressure Transducer Locations.....	5
Figure 4. Raw Acceleration Histories for 5-foot Drops.....	5
Figure 5. Filtered Acceleration Histories for 5-foot Drops.....	6
Figure 6. Raw Acceleration Histories for 10-foot Drops.....	6
Figure 7. Filtered Acceleration Histories for 10-foot Drops.....	7
Figure 8. Pressure Histories for 5-foot Drops.....	8
Figure 9. Pressure Histories for 10-foot Drops.....	8
Figure 10. Two-Dimensional Axisymmetric Model.....	10
Figure 11. Mesh Variants for Two-Dimensional Axisymmetric Model.....	11
Figure 12. Three-Dimensional Quarter Model	12
Figure 13. 0.025-inch Fluid Element Mesh Variant	13
Figure 14. Closed-Form Solution Acceleration History for 5-foot Drop	14
Figure 15. Closed-Form Solution Acceleration History for 10-foot Drop	14
Figure 16. Closed-Form Solution Pressure History for 5-foot Drop	15
Figure 17. Closed-Form Solution Pressure History for 10-foot Drop	15
Figure 18. Acceleration Histories for 5-foot Drop for 0.025-inch Element Size	16
Figure 19. Acceleration Histories for 5-foot Drop for 0.05-inch Element Size	16
Figure 20. Acceleration Histories for 5-foot Drop for 0.1-inch Element Size	17
Figure 21. Acceleration Histories for 10-foot Drop for 0.025-inch Element Size	17
Figure 22. Acceleration Histories for 10-foot Drop for 0.5-inch Element Size	18
Figure 23. Acceleration Histories for 10-foot Drop for 0.1-inch Element Size	18
Figure 24. Peak Accelerations for Mesh and Coupling Stiffness Variants for 5-foot Drops	19
Figure 25. Peak Acceleration for Mesh and Coupling Stiffness Variants for 10-foot Drops	19
Figure 26. Pressure in Fluid versus DBFSI Pressure at Coupling Surface.....	20
Figure 27. Pressure Histories for 5-foot Drop for 0.025-inch Element Size	21
Figure 28. Pressure Histories for 5-foot Drop for 0.05-inch Element Size	21
Figure 29. Pressure Histories for 5-foot Drop for 0.1-inch Element Size	22
Figure 30. Pressure Histories for 10-foot Drop for 0.025-inch Element Size	22
Figure 31. Pressure Histories for 10-foot Drop for 0.05-inch Element Size	23
Figure 32. Pressure Histories for 10-foot Drop for 0.1-inch Element Size	23
Figure 33. Pressure Histories for 5-foot Drop for 10 x Curve 10 Mesh Variants.....	24
Figure 34. Pressure Histories for 10-foot Drop for 10 x Curve 10 Mesh Variants.....	24
Figure 35. Peak Pressure for Mesh and Coupling Stiffness Variants for 5-foot Drops.....	25
Figure 36. Peak Pressure for Mesh and Coupling Stiffness Variants for 10-foot Drops.....	25
Figure 37. Impulse for Mesh and Coupling Stiffness Variants for 5-foot Drops	26
Figure 38. Impulse for Mesh and Coupling Stiffness Variants for 10-foot Drops	26
Figure 39. Pressure Contours for Coupling Stiffness Variants for 5-foot Drop	27
Figure 40. Peak Filtered Accelerations for Sensitivity Study Variants	28
Figure 41. Peak Pressures for Sensitivity Study Variants.....	29
Figure 42. Pressure Pulse Caused by a 0.02-inch Divot.....	30
Figure 43. Acceleration History for 5-foot Drop Simulations.....	31

Figure 44. Acceleration History for 10-foot Drop Simulations.....	31
Figure 45. Pressure Histories for 5-foot Drop Simulations	32
Figure 46. Pressure Histories for 10-foot Drop Simulations	33
Figure 47. Pressure Distribution at 0.001 seconds after Impact for 5-foot Drop Simulations	34
Figure 48. Pressure Distribution at 0.001 seconds after Impact for 10-foot Drop Simulations ..	35
Figure 49. Acceleration Histories for Mesh Variants for 5-foot Simulations.....	36
Figure 50. Acceleration Histories for Mesh Variants for 10-foot Simulations.....	36
Figure 51. Pressure Histories for Mesh Variants for 5-foot Simulations	37
Figure 52. Pressure Histories for Mesh Variants for 10-foot Simulations	37
Figure 53. Pressure Transducer Arrangement	38
Figure 54. Pressure Histories for Multiple Pressure Transducers.....	39
Figure 55. Description of Penetration and Leakage.....	41
Figure 56. Symptoms of an Excessively Soft Coupling Stiffness	42
Figure 57. Symptoms of Excessively High Coupling Stiffness.....	43

List of Tables

Table 1. Parameters Varied for Sensitivity Study.....	28
Table 2. Pressure Transducer Locations	38
Table 3. Pressure Pulse Width Estimate	39
Table 4. Recommendations for Element Size and Coupling Stiffness	40

1. Introduction

Spacecraft are being designed based on LS-DYNA [1] simulations of water landing impacts. The Elemental Water Impact Test (EWIT) series was undertaken to assess the accuracy of LS-DYNA water impact simulations. Phase 1 of the EWIT series featured water impact tests of a 20-inch hemisphere dropped from heights of 5 feet and 10 feet.

2. Simulations

2.1. LS-DYNA

LS-DYNA is a general purpose transient dynamic finite element code capable of simulating complex real world problems. LS-DYNA's strength is in the modeling of impact problems. An explicit time integration scheme is used in which there is no equilibrium check and iteration of the solution between time steps. This approach works only because the time step is restricted to be smaller than the shortest stress wave transit time for any element in the model.

The modeling of contact between bodies in LS-DYNA is accomplished via a penalty method. Contact is detected when the nodes of one body pass through the face or edges of the elements of another body. Preloaded penalty springs are then inserted to push the bodies apart. One consequence of this approach is one body must always penetrate another body before contact is detected. Another consequence is that there is a finite contact stiffness at the interface between the bodies that is entirely nonphysical.

LS-DYNA has a limited capability to model a fluid using Arbitrary Lagrangian-Eulerian (ALE) meshes. In the ALE approach, each time step begins with a mesh that is conceptually similar to the Lagrangian meshes used to model structures. LS-DYNA determines the deformation of the fluid that occurs during the time step, then moves, or advects, the mesh back to its original configuration and treats the fluid as having moved through the mesh. The result is that the nodes of the mesh do not move. Instead, the volume fraction of the fluid in each element is changed. The fluid in the ALE mesh can flow, compress, and impart momentum; however, the ALE mesh does not offer a full Navier-Stokes fluid flow solution.

LS-DYNA features many parameters that can be adjusted in modeling of fluid-structure interaction problems. An overarching parameter is the mesh density. As with all finite element codes, a smaller element size generally produces results that are more accurate. In addition to mesh density, there are many other solution parameters that can be selected. Several of these are discussed in the following sections.

2.2. ALE Solution Parameters

The *CONTROL_ALE card includes several parameters, most of which should be allowed to take default values. The number of solution cycles per mesh advection step, NADV, should ideally be specified as 1, though it can be set to a higher value if necessary to reduce solution time. Various options for the mesh advection method, METH, are available. The developer recommends METH=2, which is second order accurate. Other options can be tried if necessary to reduce solution time. Several parameters are available for mesh advection smoothing. The developer warns that the smoothing algorithm is not based in physics. It is recommend that smoothing be turned off, AFAC=-1.

2.3. Element Section Parameters

For a 2-D mesh, *SECTION_ALE2D offers two axisymmetric element formulations. ELFORM=14 is area weighted and ELFORM=15 is volume weighted. The code developer strongly recommends ELFORM=14. For a 3-D mesh, *SECTION_SOLID offers two treatments of an air space above a fluid. ELFORM=11 allows the air to be treated as a fluid with its own equation of state. ELFORM=12 treats the air as a void space. The code developer recommends ELFORM=11.

2.4. Material Parameters

Fluids with an equation of state utilize *MAT_NULL. The most important material property for the impact problem is the material density, RO. The tensile pressure cutoff, PC, is typically set to either zero or a very small negative number. If the air is treated as a void space (ELFORM=12), it may be desirable to set PC equal to negative one atmosphere (-14.7 psi) in order to mimic the fact that cavitation does not occur until the pressure drops to zero absolute pressure. The LS-DYNA Keyword User's Manual [2] implies that a non-zero value must be specified in order for the fluid to be able to cavitate.

2.5. Equation of State Parameters

The two most commonly used equations of state for water are *EOS_GRUNEISEN and *EOS_LINEAR_POLYNOMIAL. *EOS_GRUNEISEN is required for water at high pressure as would occur in the simulation of an underwater explosion. For the range of pressures seen in the water impact problem, the two options provide similar relationships between pressure and volumetric strain. *EOS_LINEAR_POLYNOMIAL is readily usable for both water and air.

2.6. Fluid Structure Coupling Parameters

The *CONSTRAINED_LAGRANGE_IN_SOLID card features many options. The default for the number of fluid-structure coupling points on the surface of each structural element, NQUAD, is a 2 x 2 array of coupling points. If the structural elements are larger than the fluid elements, a larger number of NQUAD points should be specified. Perhaps the most important coupling parameter is the coupling stiffness, PFAC. If PFAC is a positive value, the coupling stiffness is based on the solution time step and the mass of the nodes on either end of the penalty coupling springs. The default is PFAC=0.1. A negative value for PFAC points to a user-specified coupling stiffness curve. The curve specifies the coupling pressure as a function of the distance the fluid penetrates past the coupling surface. The user can also specify the fluid element minimum volume fraction at which coupling is activated, FRCMIN. The default is FRCMIN=0.5. Problems with excessive penetration of fluid into the structure can be addressed by reducing FRCMIN; however, there is no firm physical basis for this. Simulations with low values of FRCMIN have been observed to show the fluid moving away from the structure prematurely.

2.7. Boundary Conditions

The typical approach for modeling a water or soil block in an impact problem is to restrain the sides and bottom of the mesh in the directions normal to each face. The problem with this approach is that stress waves are reflected when they reach the mesh boundary. Usually, dispersion of the stress waves results in negligible pressure amplitude by the time the stress wave arrives back in the area of the impact. An alternative approach is to designate a layer of elements along the sides and bottom of the mesh as ambient

pressure reservoir elements. This is done via the ambient element type option, AET=4, on the *SECTION cards. The ambient pressure reservoir elements allow material to flow in and out of the mesh while holding the pressure constant.

2.8. Gravity and Atmospheric Preload

It is customary in water and soil impact problems to initialize gravity at 1g instantaneously at the start of a simulation. The result is that stress waves oscillate through the material throughout the solution duration. This typically has negligible effect on the solution as the amplitude of the pressure oscillations is similar to the hydrostatic head at the base of the mesh, which is much less than the pressure due to the impact. A more accurate method is to ramp gravity to 1g prior to the impact. The result is a stable hydrostatic stress state in the material provided that the ramp time is much longer than the time required for a stress wave to propagate through the depth of the mesh. If there is no atmospheric overpressure, the pressure in the material at the surface will be zero, which could allow material to cavitate prematurely. If the air is treated as a void (ELFORM=12), premature cavitation can be prevented by setting the tensile cutoff pressure on the *MAT_NULL input, PC, equal to negative one atmosphere (-14.7 psi). If the air is modeled as a fluid (ELFORM=11), the *INITIAL_HYDROSTATIC_ALE and *ALE_AMBIENT_HYDROSTATIC options can be used to preload the air and water meshes with atmospheric and hydrostatic pressure. For the *INITIAL_HYDROSTATIC_ALE and *ALE_AMBIENT_HYDROSTATIC options, *EOS_LINEAR_POLYNOMIAL must be used to define the equation of state for the air and water.

3. Tests

3.1. Test Configuration

The drop tests were performed in a 15-foot diameter above-ground swimming pool located in the Room 123 high-bay area of Building 1293A at NASA Langley Research Center (LaRC). The depth of the water in the pool was approximately four feet. The test pool was located inside a 24-foot diameter above-ground swimming pool to catch any over splash. A foam pad was placed under the liner at the bottom of the inner pool to cushion bottom impacts. The test article was suspended above the test pool on a boom extended from a forklift. A line hanging from the test article was used to measure the drop height. The test set-up is illustrated in Figure 1.

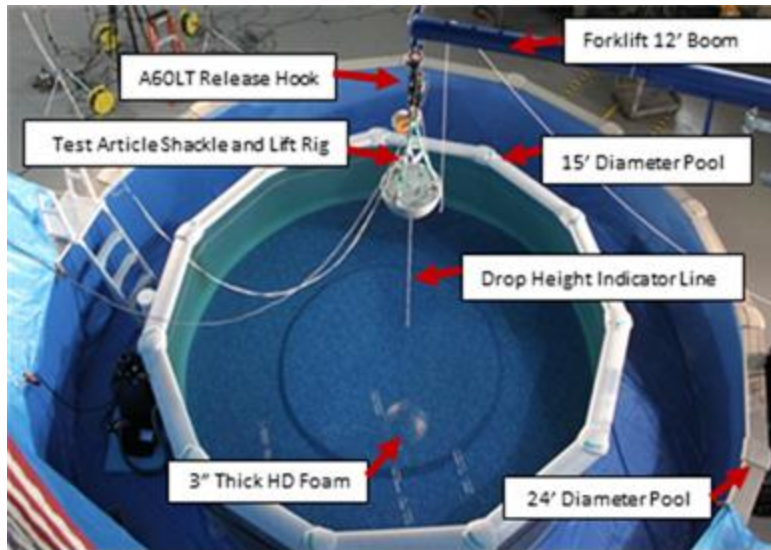


Figure 1. Test Set-Up

3.2. Test Article

The test article was a hemispherical aluminum shell with an outside diameter of 20 inches. The general configuration of the test article is illustrated in Figure 2. The hemisphere had a shell thickness of 0.19 inches and was filled with bismuth ballast to an approximate depth of 2.5 inches at the apex. Eight phenolic ribs served as internal attachment points for instrumentation, which included an accelerometer at the center and three pressure transducers at a distance of approximately 2.25 inches from the apex. The locations of the pressure transducers are illustrated in Figure 3. An aluminum lid with a thickness of 0.25 inches served to keep water away from the instrumentation. The hemisphere was lifted into position for the drop test via three lift points at the perimeter of the lid. The weight of the hemisphere with instrumentation was 48 lb.



Figure 2. Hemisphere Configuration

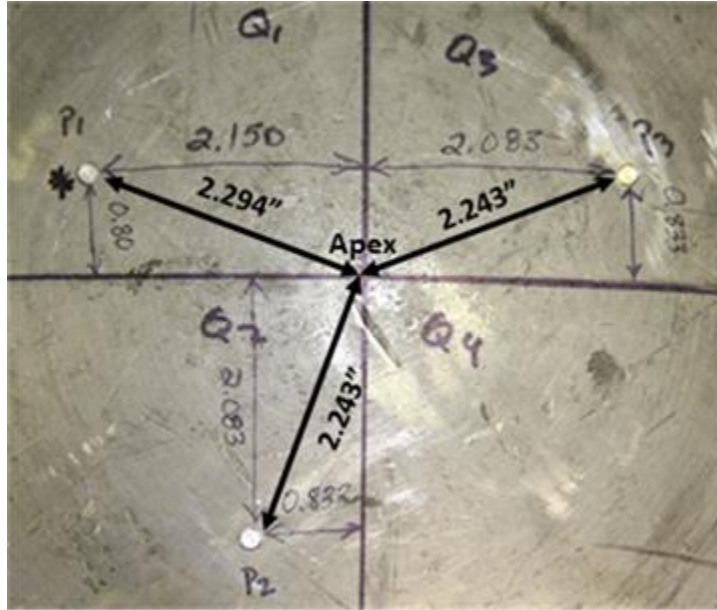


Figure 3. Pressure Transducer Locations

3.3. Test Results

Three tests were performed at a 5-foot drop height and three were performed at a 10-foot drop height. For comparison with simulation data, the acceleration histories were filtered using a 180 Hz Butterworth filter to remove the vibratory structural response. Figures 4 and 5 show raw and filtered acceleration histories for the 5-foot drops. Figures 6 and 7 show the acceleration histories for the 10-foot drops. An artifact of the filtering is a small negative dip in acceleration prior to impact.

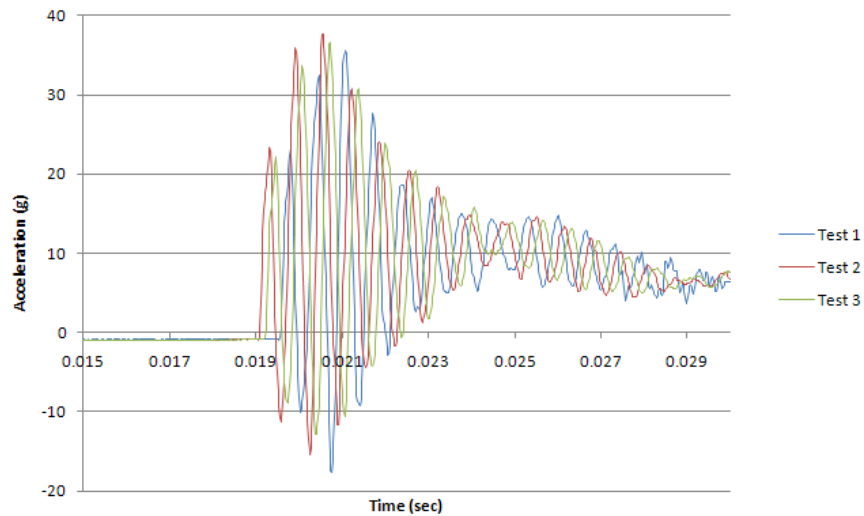


Figure 4. Raw Acceleration Histories for 5-foot Drops

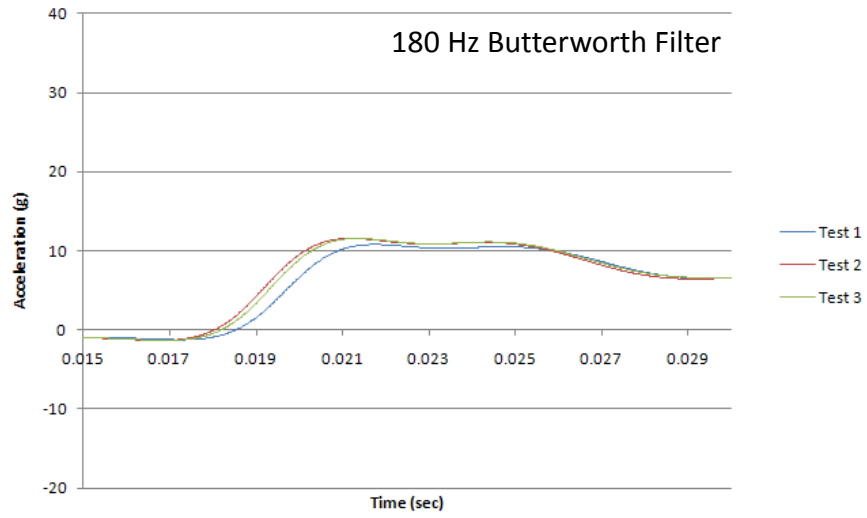


Figure 5. Filtered Acceleration Histories for 5-foot Drops

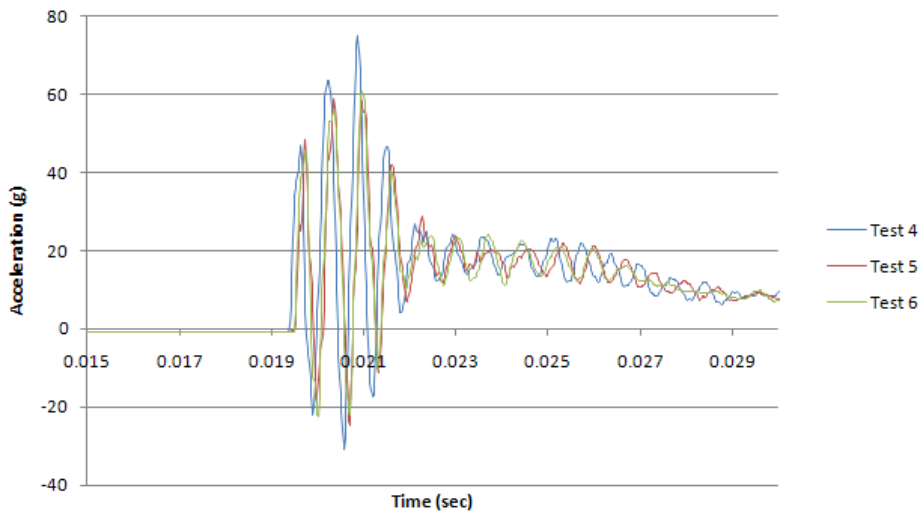


Figure 6. Raw Acceleration Histories for 10-foot Drops

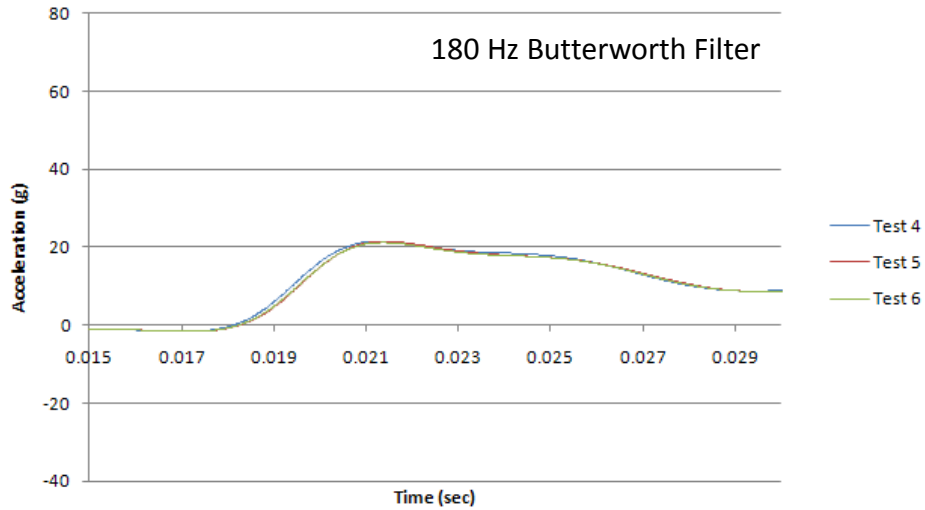


Figure 7. Filtered Acceleration Histories for 10-foot Drops

Histories from the pressure transducers for the 5-foot and 10-foot drops are shown in Figures 8 and 9. The sampling rate for both pressure and acceleration data was 50,000 Hz. The TDAS PRO data acquisition system used for the tests is equipped with an analog anti-aliasing filter with a cutoff frequency of 4300 Hz. The anti-aliasing filter can be bypassed, but it was used for these tests. The sampling rate was relatively high for this type of test; however, the duration of the pressure peaks is so short that even this relatively high sampling rate provides just a few points to define the pressure peaks. As a consequence, some of the pressure histories exhibit truncated peaks. Even for the pressure histories that do not show truncated peaks, it is inevitable that the data points sampled during the test did not capture the absolute pressure peak.

One pressure history from each test that does not show a truncated peak was chosen for comparison against simulation data. The chosen pressure histories are Gage 3 of Test 1, Gage 3 of Test 2, and Gage 2 of Test 3 for the five-foot drops, and Gage 1 of Test 4, Gage 2 of Test 5, and Gage 3 of Test 6 for the ten-foot drops. The peaks of the pressure histories do not occur simultaneously due to small angles of pitch that exist upon impact of the hemisphere with the water. In the figures, the relative timings of the peaks are as they occurred during the test. For comparisons between tests, the pressure histories have been arbitrarily shifted so that several peaks from different tests align.

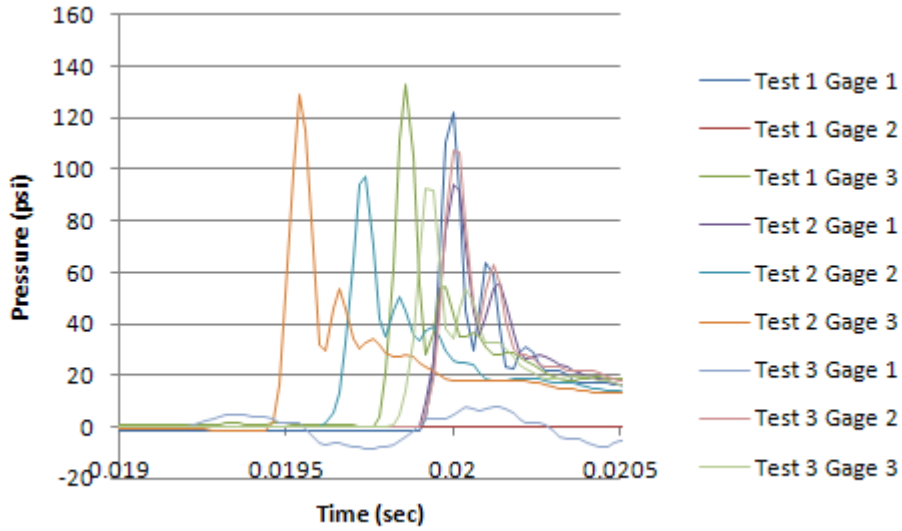


Figure 8. Pressure Histories for 5-foot Drops

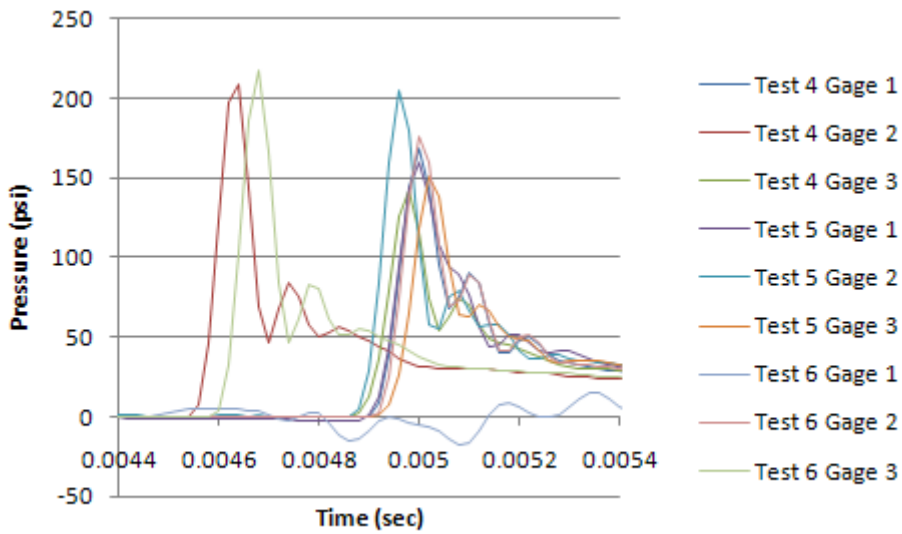


Figure 9. Pressure Histories for 10-foot Drops

4. Simulation Models

4.1. Closed-Form Solution

A closed-form solution for the acceleration and pressure histories of a sphere impacting water was developed by A.P. Cappelli and J.P.D. Wilkinson [3]. The equations are as follows.

$$A = - \left(4 \sqrt{2} \rho \frac{V_0^{5/2} R^{3/2} t^{1/2}}{M} \right) (1 + \gamma)^{-2} \quad \text{Equation 1}$$

$$P = \frac{\sqrt{2} \rho V_0^{3/2} R^{1/2} \left[1 - \gamma \left(2 - \frac{3r^2}{c^2} \right) \right]}{\pi t^{1/2} \left(1 - \frac{r^2}{c^2} \right)^{1/2} (1 + \gamma)^2} - \frac{\rho V_0^2}{2(1 + \gamma)^2} \left[1 + \frac{4r^2}{2c^2} \left(1 - \frac{r^2}{c^2} \right)^{-1} \right] \quad \text{Equation 2}$$

$$c = (2 R V_0 t)^{1/2} \quad \text{Equation 3}$$

$$\gamma = \frac{8\sqrt{2}\rho(RV_0t)^{3/2}}{3M} \quad \text{Equation 4}$$

Where:

- A = Acceleration
- P = Pressure
- ρ = Water Mass Density
- V_0 = Initial Velocity
- M = Mass
- R = Radius of Curvature at Impact Point
- r = Polar Distance from Impact Point
- c = Maximum Radius of Wetted Shell Surface
- t = Time after Impact
- γ = Non-Dimensional Parameter

Cappelli and Wilkinson note problems with Equation 2. The predicted pressure is singular at the time that the contact patch radius, c, reaches the polar distance, r, which results in the equation producing no real answer for the highest pressure at a given polar distance. Cappelli and Wilkinson recommend dropping the second term of the pressure equation as it is small everywhere except for a negative singularity at the perimeter of the contact patch. Cappelli and Wilkinson further note that the remaining term of the pressure equation predicts nonphysical negative pressure in the late time.

4.2. 2-D LS-DYNA Simulation

A model of a two-dimensional axisymmetric slice of the penetrometer was used to evaluate the sensitivity of the acceleration and pressure to several LS-DYNA parameters. The model configuration is illustrated in Figure 10.

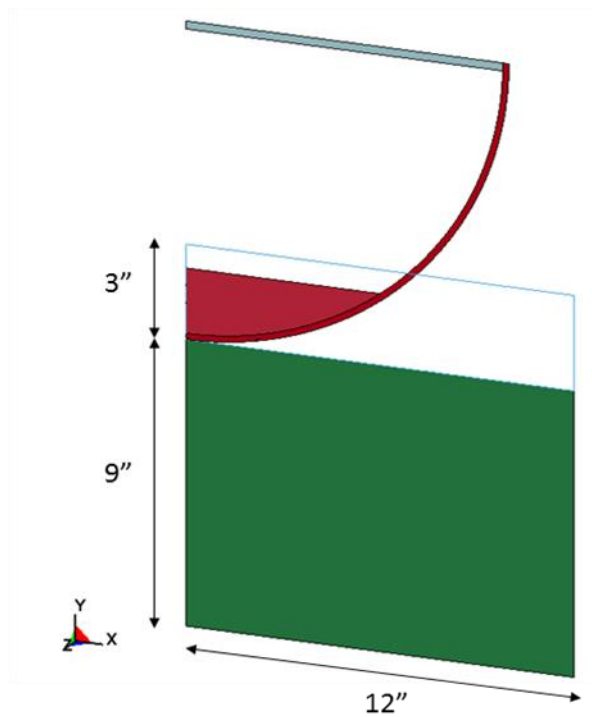


Figure 10. Two-Dimensional Axisymmetric Model

The hemisphere was treated as linear elastic. Aluminum material properties were specified for the shell and the cover. The internal ballast was bismuth. The material density of the bismuth ballast was adjusted to achieve the desired total weight of 48 lb. The water was modeled with an equation of state. The air was treated as a vacuum. Gravity was ramped to 1g during the first 0.01 seconds to obtain a stable hydrostatic pressure state in the water prior to impact. The initial height and velocity of the hemisphere were adjusted so that impact occurred at the desired velocity at 0.01 seconds. The LS-DYNA cards that describe the coupling stiffness, material properties, and initial conditions are provided in Appendix A.

Three mesh variants of the model were used with element edge lengths of 0.1, 0.05, and 0.025 inches in the area of the initial contact for both the hemisphere shell and the water. The meshes are illustrated in Figure 11.

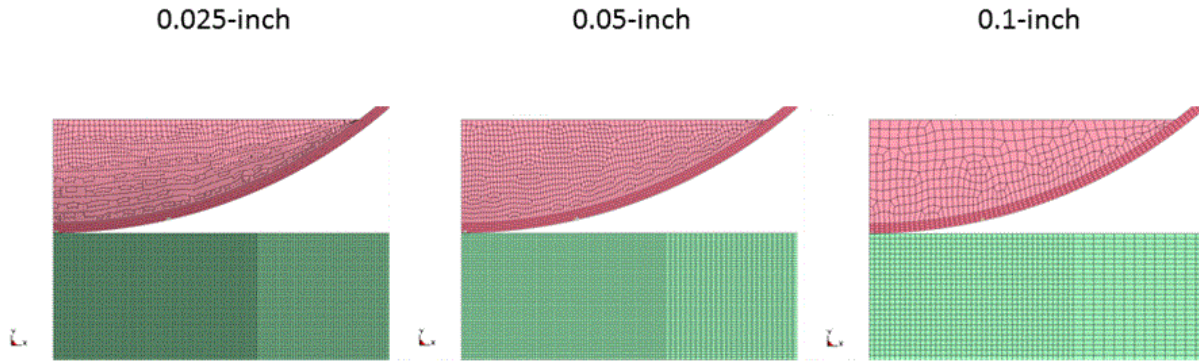


Figure 11. Mesh Variants for Two-Dimensional Axisymmetric Model

The pressure transducers used for the tests had a diameter of approximately one-eighth inch. For the simulations, coupling pressure was recorded using the DBFSI option in LS-DYNA. The pressure was averaged for the elements that span 0.1 inches at the pressure transducer location. This was one element for the 0.1-inch mesh, two elements for the 0.05-inch mesh, and four elements for the 0.025-inch mesh.

The baseline coupling stiffness was designated Curve 10. Curve 10 featured 100 psi at a penetration of 0.005 inches. Simulations were also performed with variants of Curve 10 with the stiffness scaled by factors of 0.1, 10, and 100.

4.3. 3-D LS-DYNA Simulation

A three-dimensional quarter model of the hemisphere was used for further evaluations of coupling stiffness and mesh density. The three-dimensional model was considered necessary because the 2-D and 3-D sections of the LS-DYNA code were written by different developers. The theory is the same for both, but there is no certainty that the implementation behaves in exactly the same manner, so there is no certainty that the findings concerning one modeling approach are directly applicable to the other. The three-dimensional model is illustrated in Figure 12.

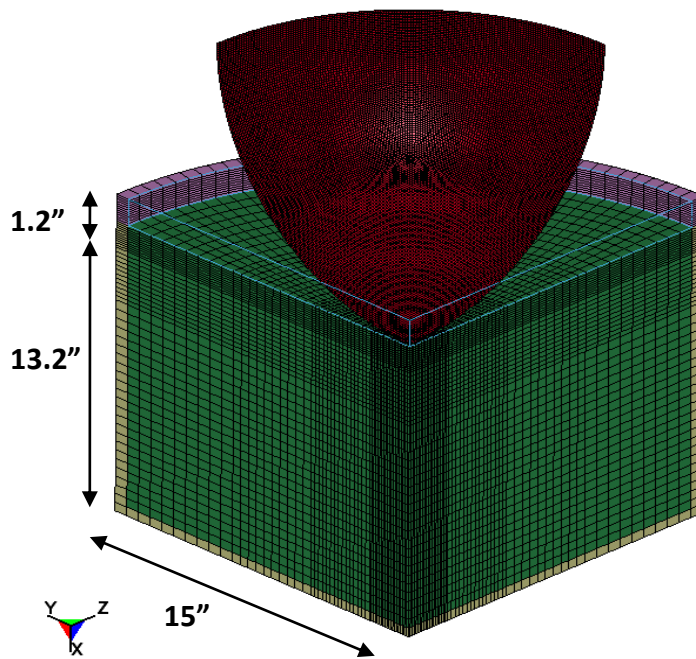


Figure 12. Three-Dimensional Quarter Model

The hemisphere was treated as rigid. Both the air and the water were modeled with equations of state. Gravity was initiated instantaneously and options within LS-DYNA were employed to initiate the air at one atmosphere and the water at one atmosphere plus hydrostatic pressure. The initial height of the hemisphere above the water was set so that impact occurred immediately after the start of the simulation. The bottom and outermost layers of elements of the water and air meshes were defined as reservoir elements. The reservoir elements allow material to flow in or out of the mesh in order to maintain constant pressure at the boundary. The LS-DYNA cards that describe the coupling stiffness, material properties, and initial conditions are provided in Appendix B.

Three water meshes were used. The baseline mesh featured an element size of 0.1 inches near the initial impact. The overall mesh radius was 15 inches, the air height was 1.2 inches, and the water depth was 13.2 inches. The first variant featured an element size of 0.05 inches near the initial impact and the same overall mesh radius and depth as the baseline mesh. The second variant was created by halving the dimensions of the 0.05-inch mesh. This resulted in an element size of 0.025 inches near the initial impact and an overall mesh radius of 7.5 inches, an air height of 0.6 inches, and a water depth of 6.6 inches. The 0.025-inch element model is illustrated in Figure 13. Due to the limited extent of the mesh, the 0.025-inch element model was suitable only for short duration simulations to determine early-time impact response.

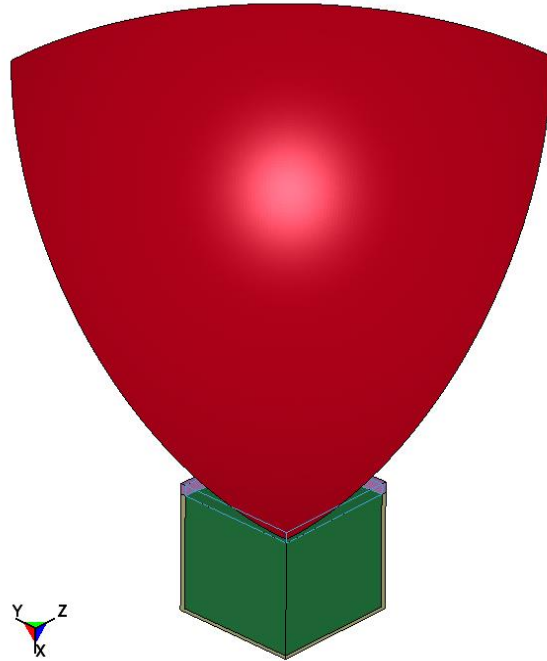


Figure 13. 0.025-inch Fluid Element Mesh Variant

For all simulations, the element size for the hemisphere was 0.1 inches, which is similar to the size of the pressure transducer used in the tests. Pressures from the simulations were recorded for a single element using the DBFSI option.

The baseline coupling stiffness was designated Curve 12. Curve 12 featured 100 psi at a penetration of 0.01 inches. This was half the stiffness of the baseline Curve 10 used for the 2-D simulations. The rationale for halving the coupling stiffness for the 3-D simulations was that the baseline 3-D mesh featured elements with edge lengths twice as large as the baseline 2-D mesh. For the baseline mesh with an element size of 0.1 inches, simulations were performed with variants of Curve 12 that were scaled by factors of 0.1 and 10 for the stiffness. Simulations were also performed with the coupling stiffness default, PFAC = 0.1. LS-DYNA determines the default coupling stiffness based on the stiffness required to achieve a vibration period equal to the critical time step size for solution stability.

5. Test and Simulation Correlation

5.1. Closed-Form Results

Accelerations for the closed-form solution for the 5-foot and 10-foot drops are plotted with test data in Figures 14 and 15. The test data was filtered using a 180-Hz Butterworth filter to eliminate vibratory structural response not represented in the analytical models. The closed-form solution exhibits no noise and requires no filtering. The results show that the closed-form solution substantially over predicted the peak acceleration. This is partly due to the closed-form solution not taking into account the reduction in the velocity that occurs as a consequence of the deceleration during the early stages of the impact. For the 5-foot drop, the velocity would have reduced from 215 in/sec at impact to 168 in/sec at 0.01 seconds after impact. For the 10-foot drop, the velocity would have reduced from 304 in/sec to 206 in/sec.

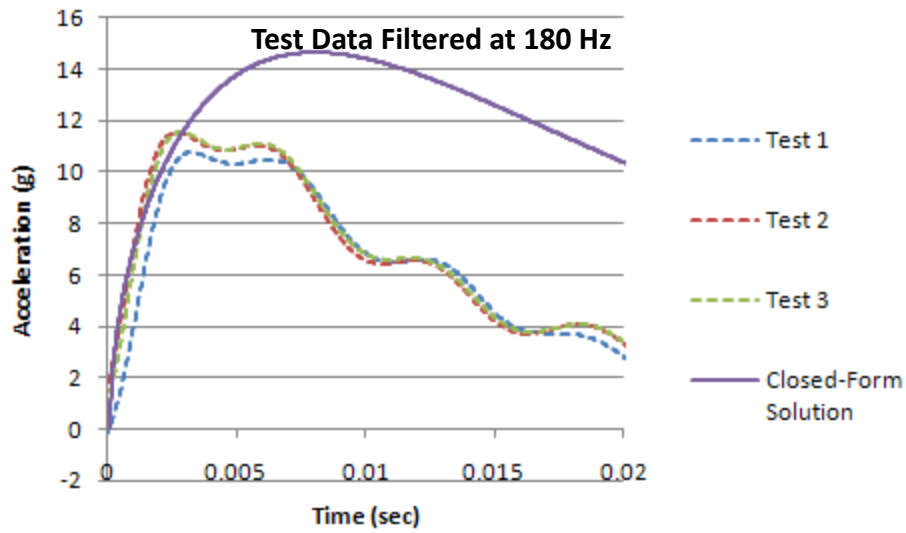


Figure 14. Closed-Form Solution Acceleration History for 5-foot Drop

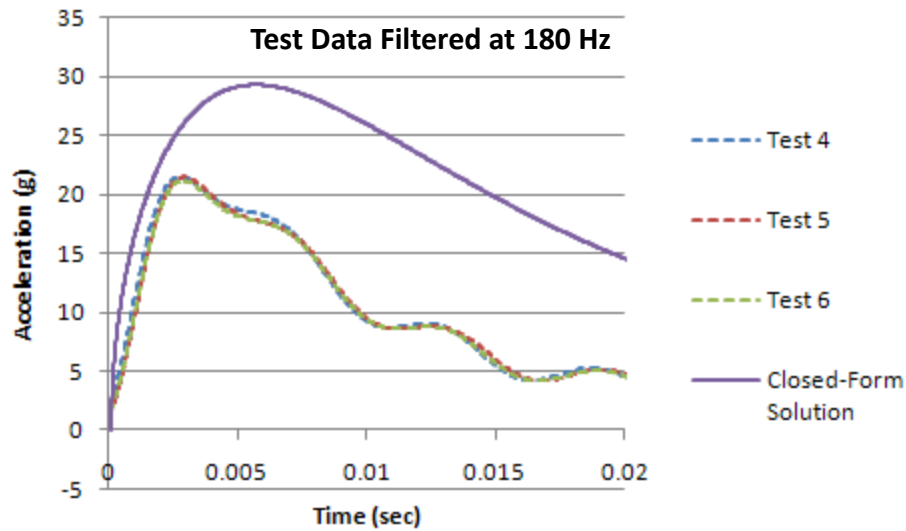


Figure 15. Closed-Form Solution Acceleration History for 10-foot Drop

The closed-form solution pressure histories are plotted with test data in Figures 16 and 17. The closed-form solution is asymptotic at the perimeter of the contact patch, but provides a reasonable prediction of the pressure decay.

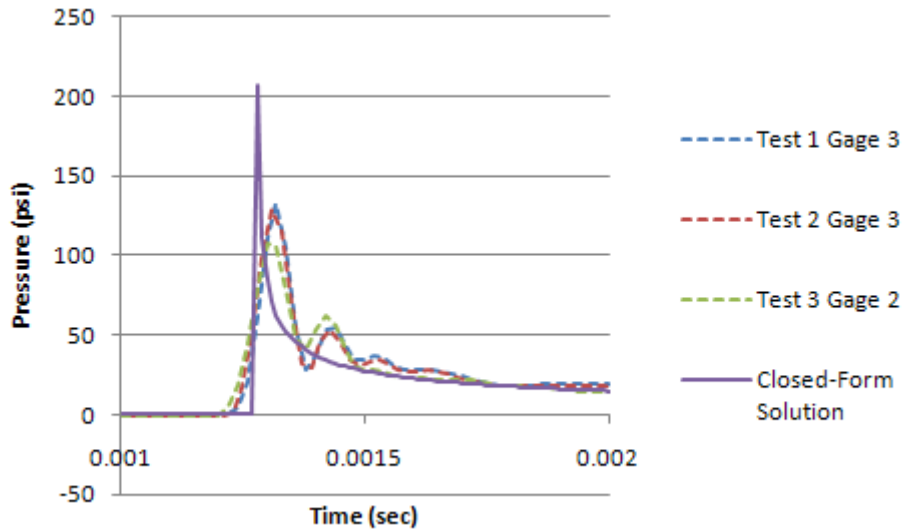


Figure 16. Closed-Form Solution Pressure History for 5-foot Drop

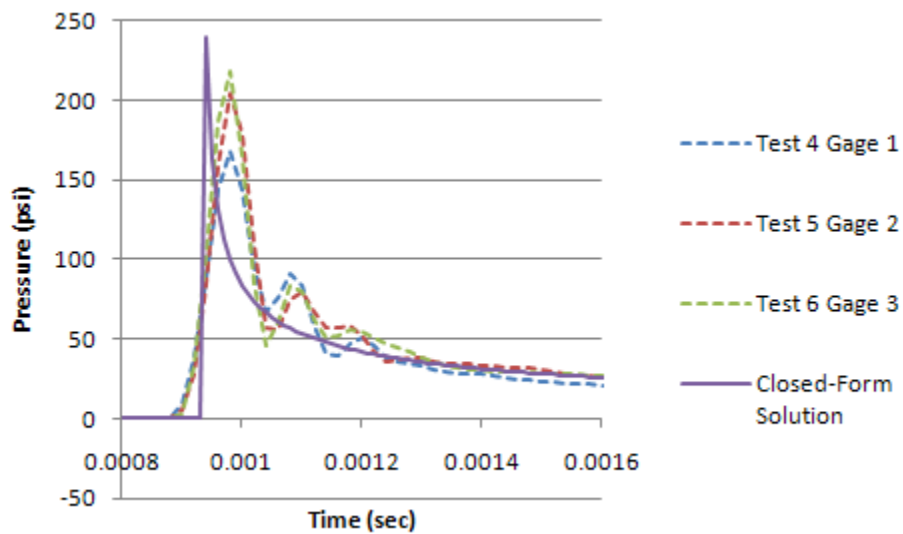


Figure 17. Closed-Form Solution Pressure History for 10-foot Drop

5.2. 2-D LS-DYNA Results

Acceleration histories for the three mesh variants are compared to test accelerometer histories in Figures 18 through 20 for the 5-foot drops and Figures 21 through 23 for the 10-foot drops. All acceleration histories were filtered using a 180-Hz Butterworth filter and were time-shifted to facilitate comparison. The figures for the 5-foot drops show close agreement with the test results. For the 10-foot drops, the simulations over-predicted the acceleration peak. Both the 5-foot and 10-foot drops show the simulations had a much slower acceleration decay rate in the late time, after approximately 0.008 seconds.

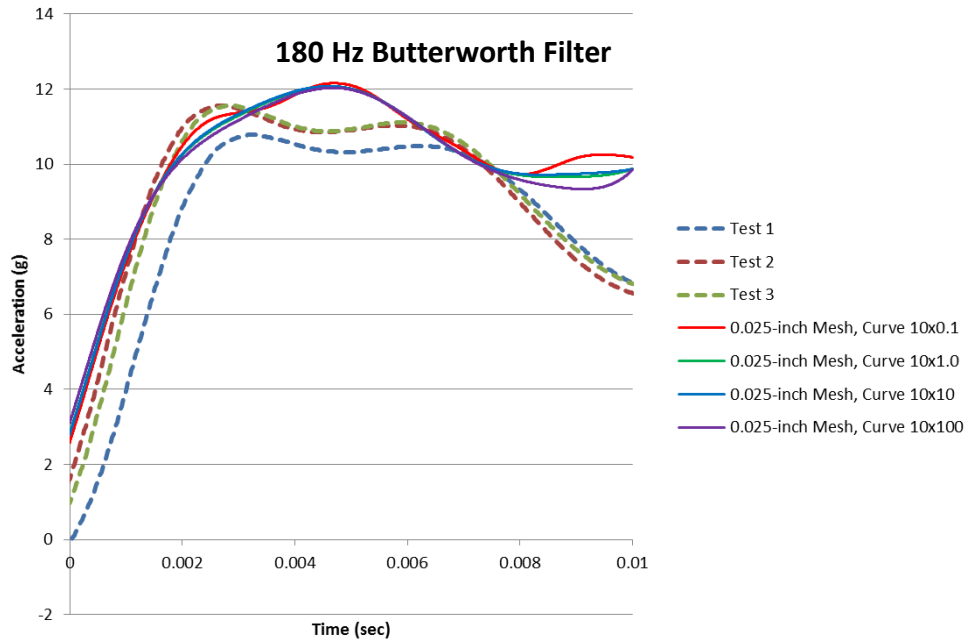


Figure 18. Acceleration Histories for 5-foot Drop for 0.025-inch Element Size

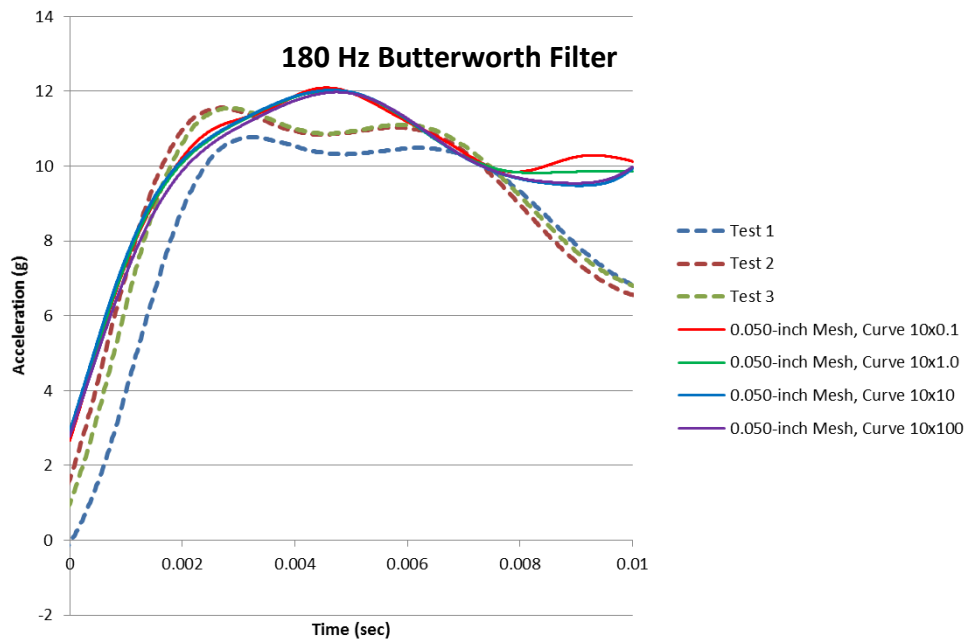


Figure 19. Acceleration Histories for 5-foot Drop for 0.05-inch Element Size

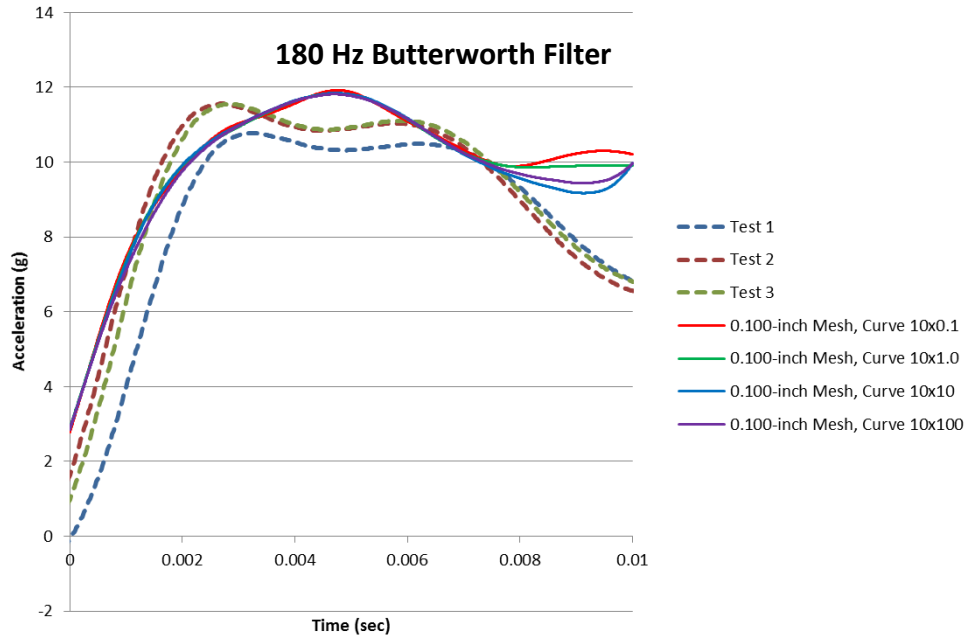


Figure 20. Acceleration Histories for 5-foot Drop for 0.1-inch Element Size

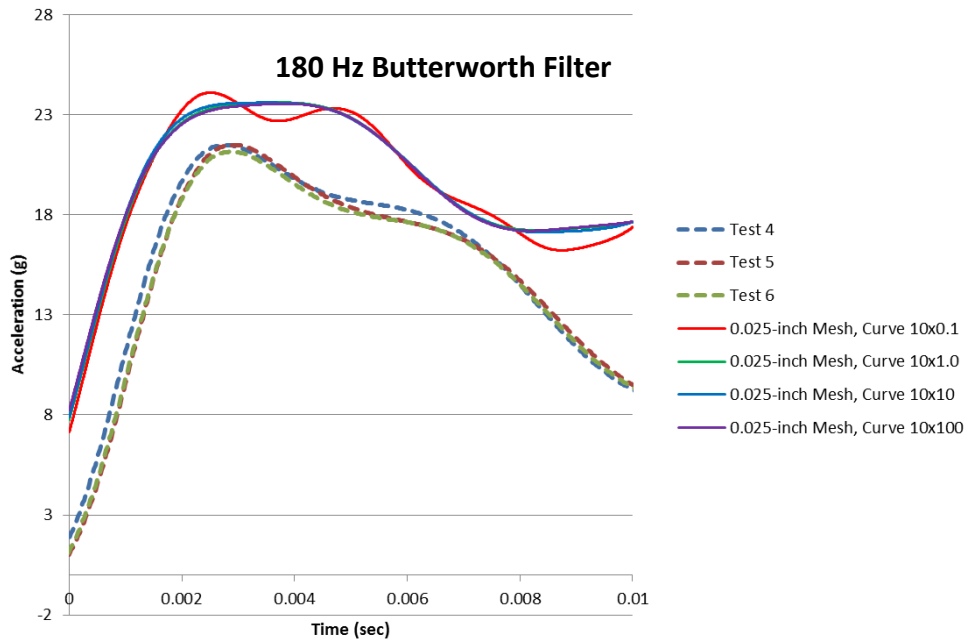


Figure 21. Acceleration Histories for 10-foot Drop for 0.025-inch Element Size

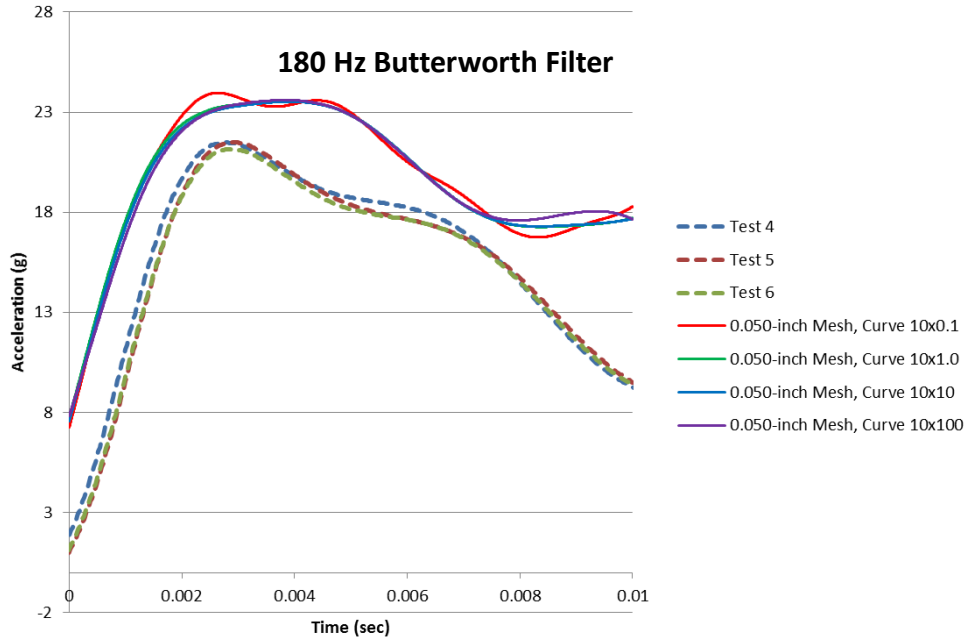


Figure 22. Acceleration Histories for 10-foot Drop for 0.5-inch Element Size

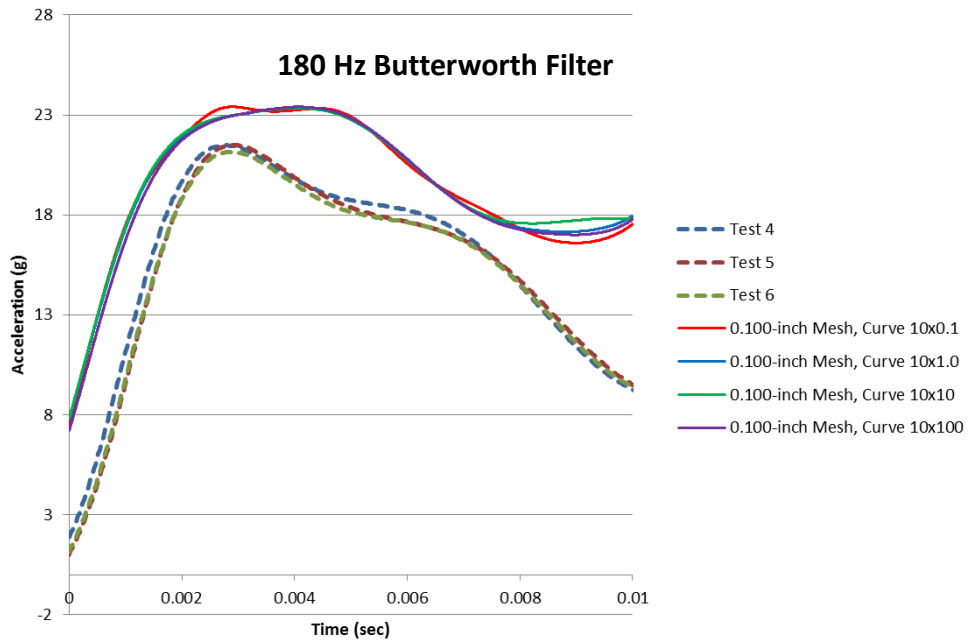


Figure 23. Acceleration Histories for 10-foot Drop for 0.1-inch Element Size

The acceleration histories show that the filtered peak acceleration is relatively insensitive to both the mesh density and the coupling stiffness for the range of element sizes and coupling stiffnesses considered. This is illustrated in the bar charts shown in Figure 24 for the 5-foot drops and Figure 25 for the 10-foot

drops. The tests produced filtered peaks of approximately 11g for the 5-foot drops and 22g for the 10-foot drops.

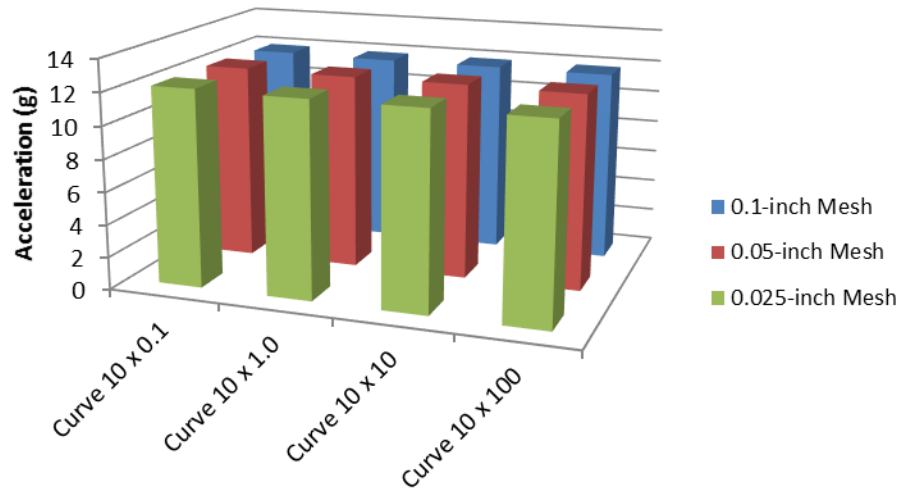


Figure 24. Peak Accelerations for Mesh and Coupling Stiffness Variants for 5-foot Drops

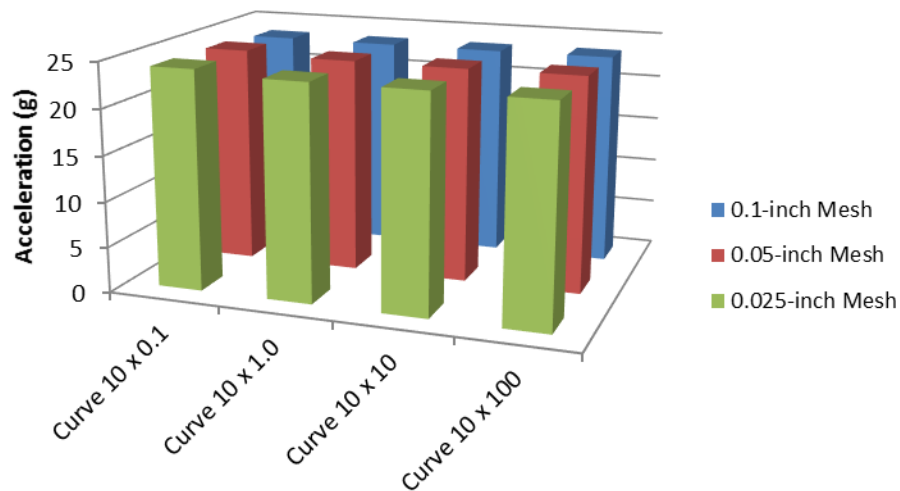


Figure 25. Peak Acceleration for Mesh and Coupling Stiffness Variants for 10-foot Drops

Pressure histories were extracted from the LS-DYNA simulations using the DBFSI option, which translates the coupling forces into an interface pressure. The DBFSI pressure does not necessarily match the pressure seen in the fluid. This is illustrated in Figure 26 for a 5-foot drop of the 0.025-inch mesh model with the 10 x Curve 10 coupling stiffness. The DBFSI pressure reflects the actual loading on the coupling surface whereas the fluid pressure represents the pressure at the center of the elements of the fluid mesh. The relative mesh densities for the fluid and structure along with the density of the fluid

coupling points on the structure (NQUAD) all factor into how closely the pressure in the fluid matches the interface pressure. Further mesh refinement would lead to better agreement between the pressure in the fluid and the pressure at the coupling surface.

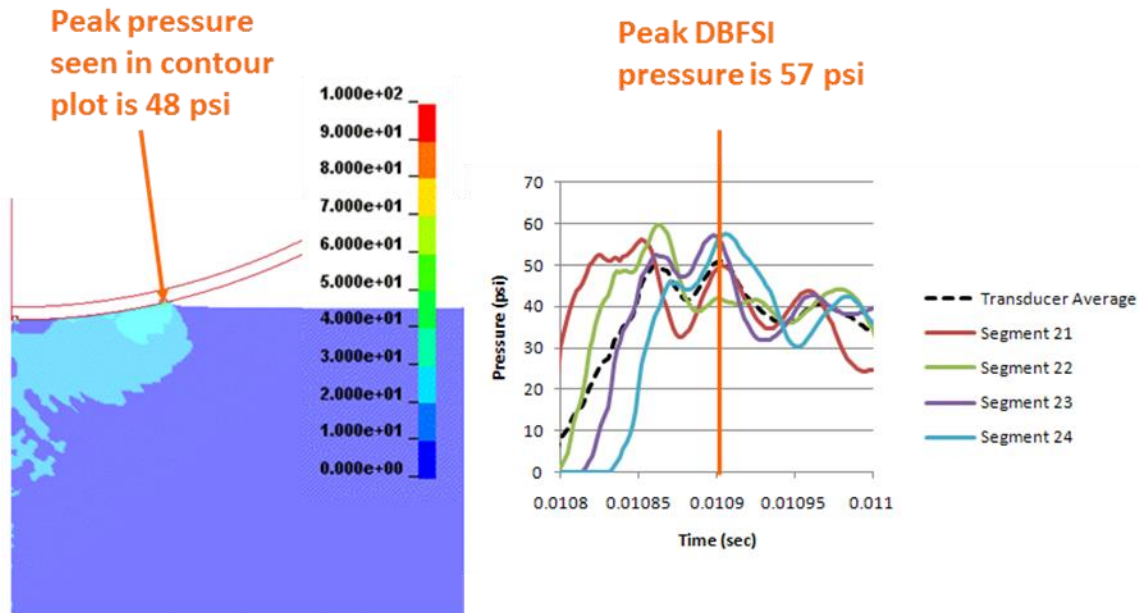


Figure 26. Pressure in Fluid versus DBFSI Pressure at Coupling Surface

Pressure histories for the three mesh variants are compared to test pressure histories in Figures 27 through 29 for the 5-foot drops and Figures 30 through 32 for the 10-foot drops. The pressure histories are unfiltered. Pressure histories for the 10 x Curve 10 simulations are shown in Figure 33 for the 5-foot drops and Figure 34 for the 10-foot drops. The simulation pressure histories have been averaged over an edge length of 0.1 inches, which approximates the pressure transducer size of 0.125 inches. The simulation results show that refining the mesh results in better agreement with the test data for the late time decay of the pressure history; however, there is no convergence in matching the peak pressure of the test data.

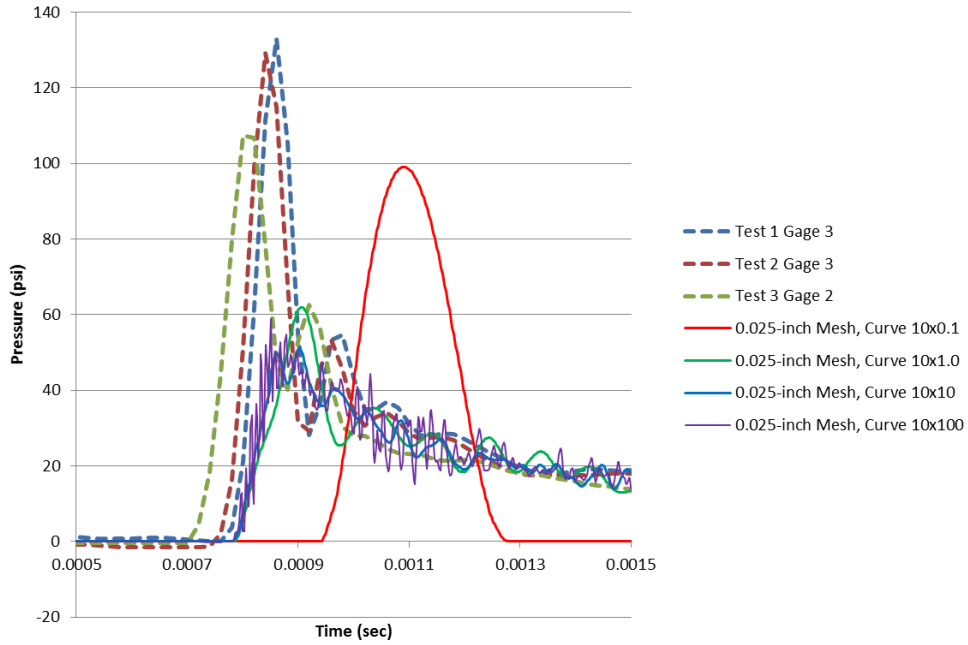


Figure 27. Pressure Histories for 5-foot Drop for 0.025-inch Element Size

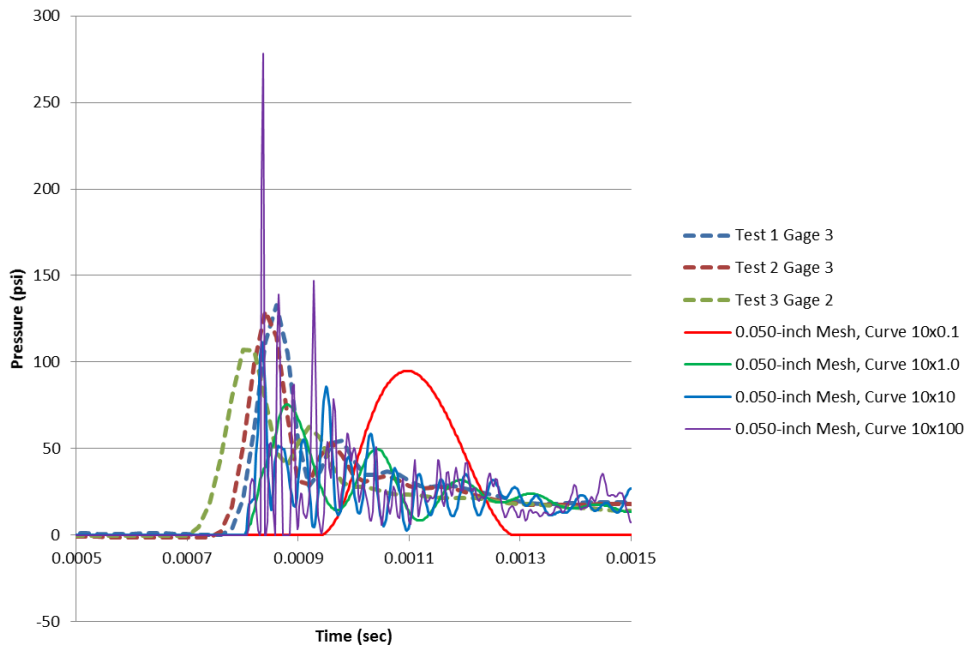


Figure 28. Pressure Histories for 5-foot Drop for 0.05-inch Element Size

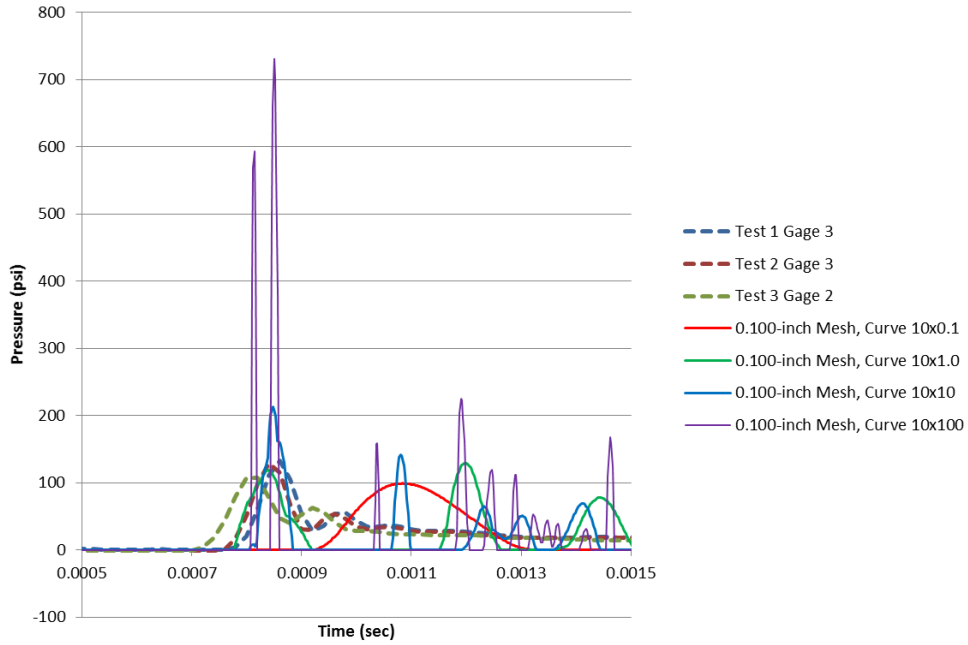


Figure 29. Pressure Histories for 5-foot Drop for 0.1-inch Element Size

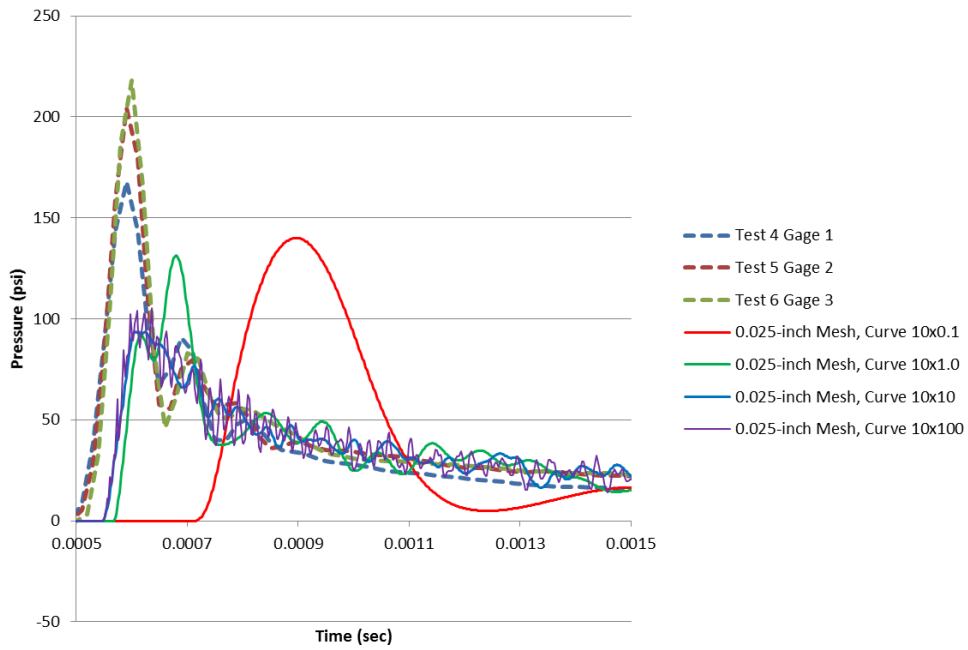


Figure 30. Pressure Histories for 10-foot Drop for 0.025-inch Element Size

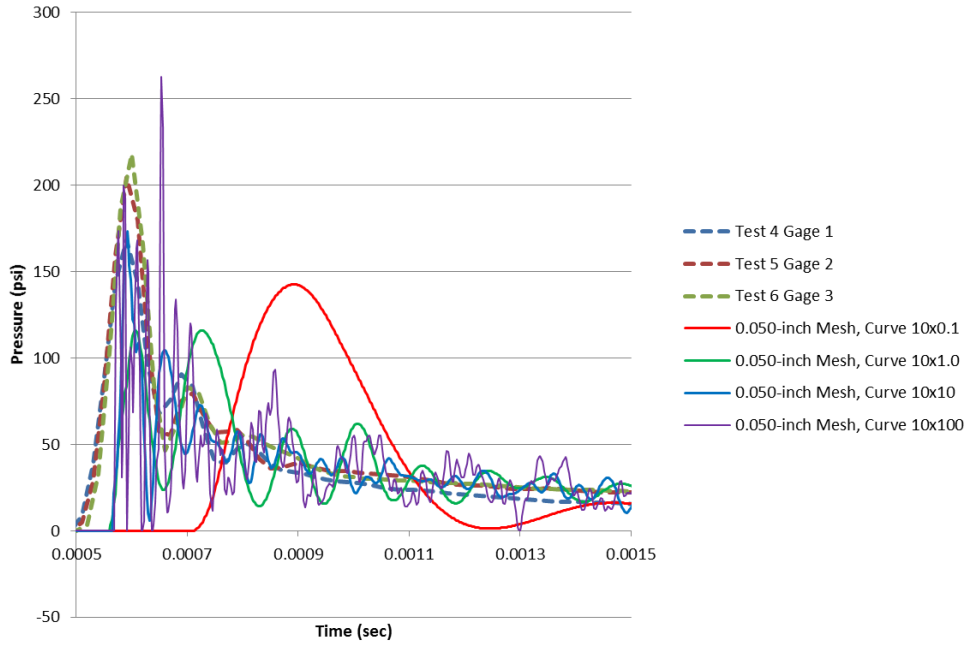


Figure 31. Pressure Histories for 10-foot Drop for 0.05-inch Element Size

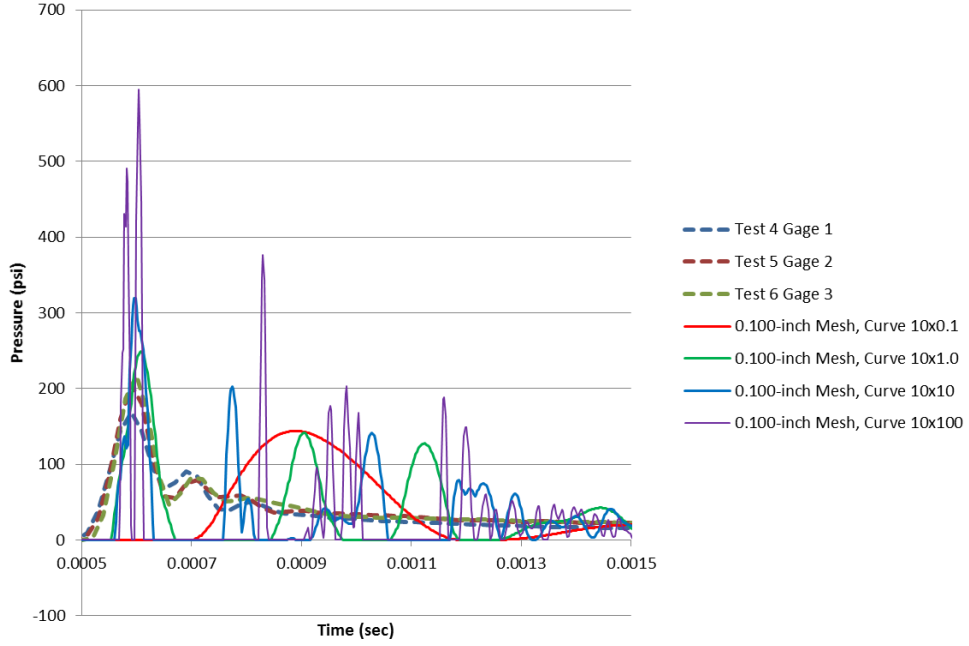


Figure 32. Pressure Histories for 10-foot Drop for 0.1-inch Element Size

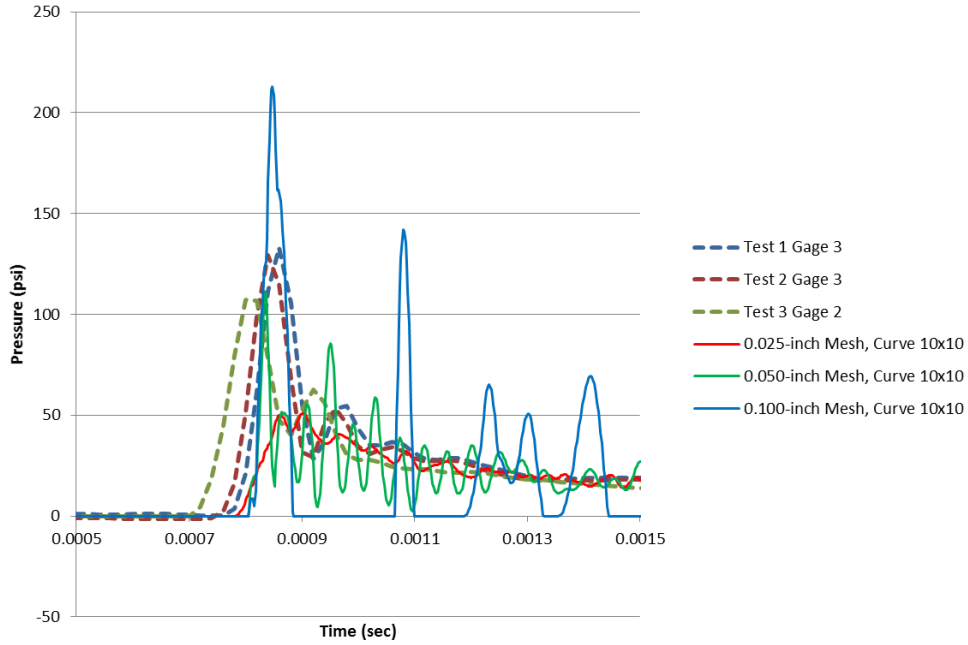


Figure 33. Pressure Histories for 5-foot Drop for 10 x Curve 10 Mesh Variants

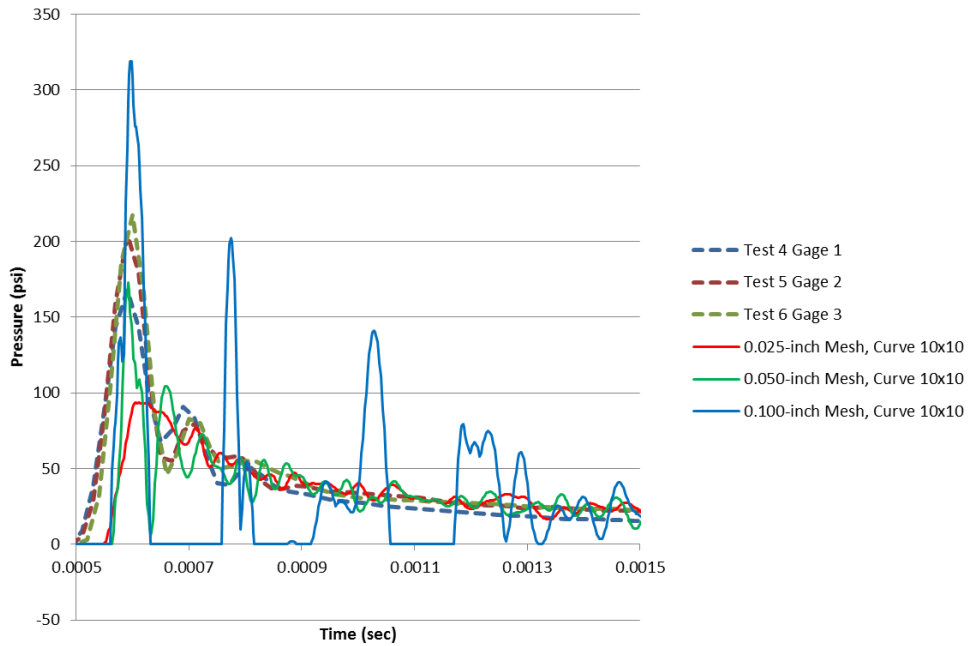


Figure 34. Pressure Histories for 10-foot Drop for 10 x Curve 10 Mesh Variants

The pressure histories show that the peak pressure is highly sensitive to both the mesh density and the coupling stiffness. The results also show that this sensitivity is reduced as the mesh is refined; however, this does not mean that the peak pressures from the simulations converge toward the peak pressures from the test. This is illustrated in the bar charts shown in Figure 35 for the 5-foot drops and Figure 36 for the

10-foot drops. The tests produced peak pressures of approximately 120 psi for the 5-foot drops and 200 psi for the 10-foot drops.

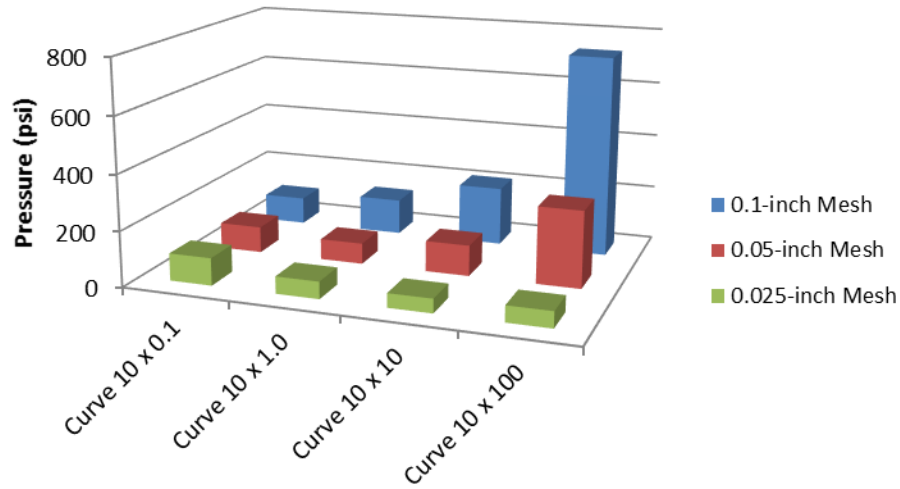


Figure 35. Peak Pressure for Mesh and Coupling Stiffness Variants for 5-foot Drops

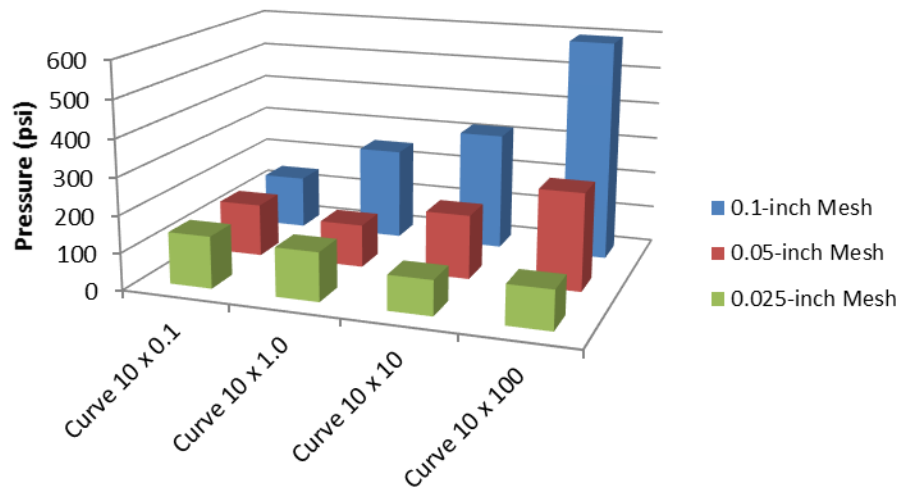


Figure 36. Peak Pressure for Mesh and Coupling Stiffness Variants for 10-foot Drops

Figures 37 and 38 show the impulse at the pressure transducer locations from the LS-DYNA simulations. The impulse was calculated by integrating the pressure history for the first 0.01 seconds following impact. Despite the drastic differences in the shapes of the pressure histories, the impulse is relatively insensitive to the mesh density and the coupling stiffness. The impulse varies between 0.069 psi-sec and 0.073 psi-sec for the simulations of the 5-foot drops and between 0.112 psi-sec and 0.117 psi-sec for the simulations of the 10-foot drops. This explains why the acceleration histories were very similar despite drastic

differences in the pressure histories. For simulation of the response of the overall structure, the exact profile of the pressure pulse is probably not important as long as the impulse is correct; however, the profile of the pressure pulse may be important for the design of small penetrations or crushable materials.

A similar computation was performed for the pressure histories from the tests. The impulse for the 5-foot drops was 0.116 psi-sec for Gage 3 of Test 1 and 0.084 psi-sec for Gage 3 of Test 2. The impulse for the 10-foot drops was 0.122 psi-sec for Gage 2 of Test 5 and 0.119 psi-sec for Gage 3 of Test 6. The pressure histories for Gage 2 of Test 3 and Gage 1 of Test 4 were not long enough to determine the impulse for the full period.

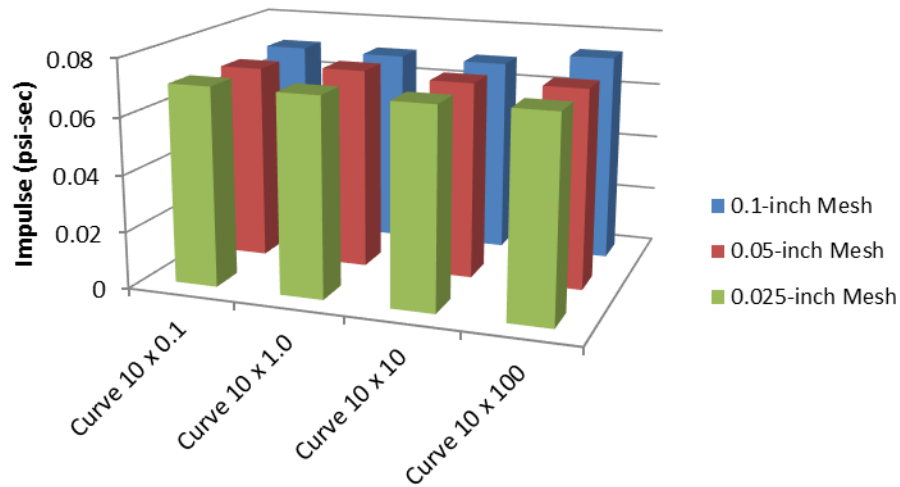


Figure 37. Impulse for Mesh and Coupling Stiffness Variants for 5-foot Drops

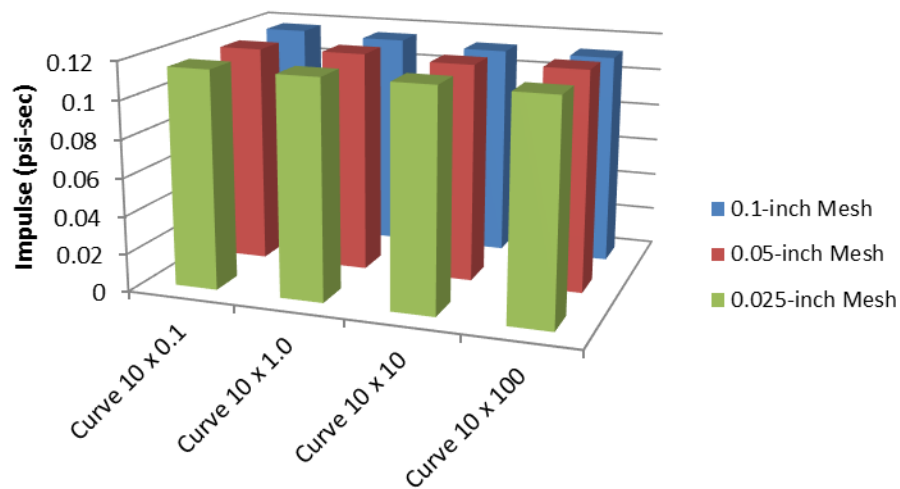


Figure 38. Impulse for Mesh and Coupling Stiffness Variants for 10-foot Drops

In addition to the effect the coupling stiffness has on the peak of the pressure history, it also affects the shape of the pressure contours within the fluid. Also, a coupling stiffness that is too soft can result in substantial penetration of fluid through the fluid-structure interface. This is illustrated in Figure 39 for the simulation of a 5-foot drop of the 0.05-inch mesh. The 0.1 x Curve 10 coupling stiffness produces smooth pressure contours but shows significant penetration of the fluid into the structure. The 100 x Curve 10 coupling stiffness shows no penetration, but the pressure contours show multiple isolated patches of high pressure. For the 100 x Curve 10 coupling stiffness, the impact occurs as a series of localized hits rather than as one continuous impact.

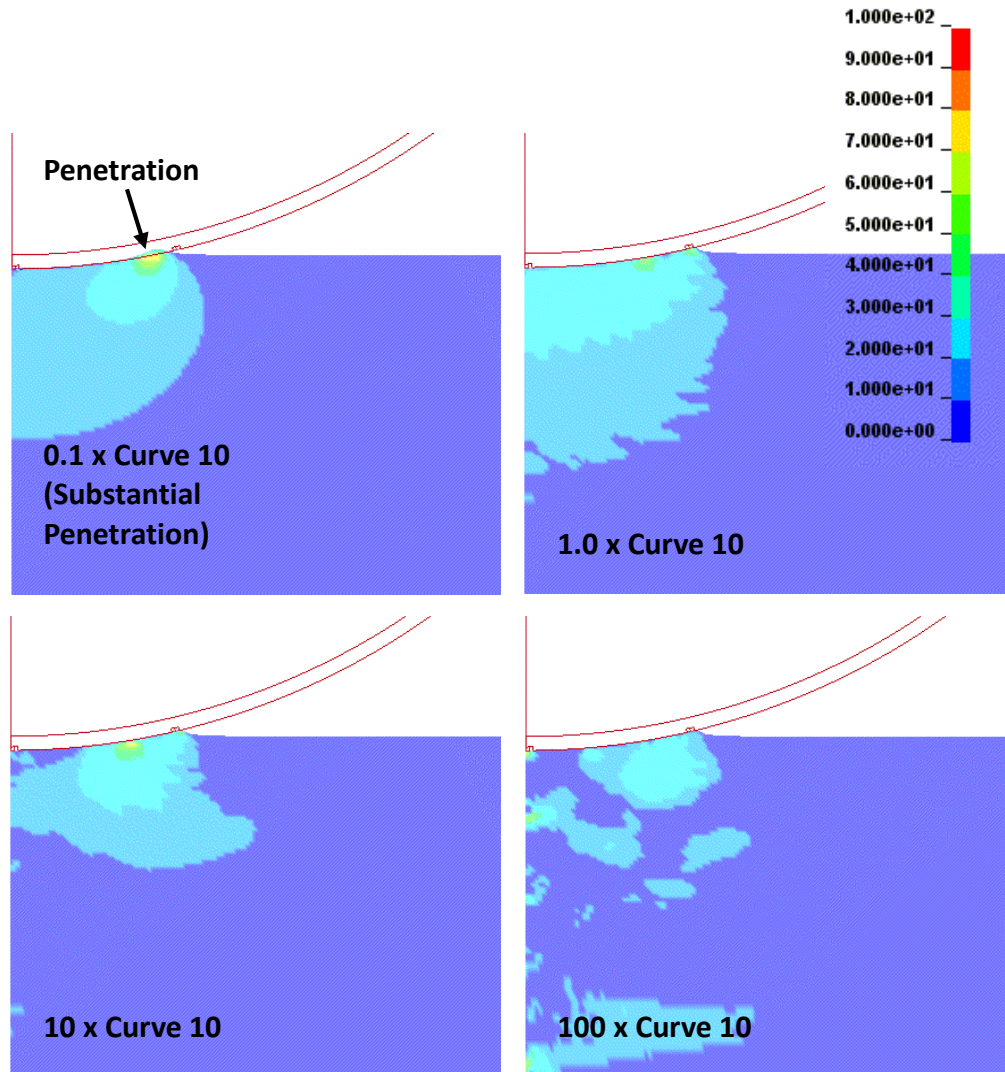


Figure 39. Pressure Contours for Coupling Stiffness Variants for 5-foot Drop

Sensitivity studies were performed for several simulation parameters. The parameters varied are listed in Table 1. The baseline simulation for the study was the 0.05-inch element model dropped from 5 feet. An exception was made for the divot model, which was based on the 0.025-inch element model in order to provide a finer mesh for defining the divot. Bar charts illustrating the peak filtered acceleration and peak

pressure are shown in Figures 40 and 41. Most of these parameters had relatively little effect on the peak filtered acceleration and peak pressure.

Table 1. Parameters Varied for Sensitivity Study

Parameter	Description	Baseline
ELFORM	Element formulation for 2-D axisymmetric mesh.	14
EOS_GRUNEISEN	Form of the equation of state for the water.	EOS_LINEAR_POLYNOMIAL
FRCMIN	Volume fraction at which a fluid element is considered to be coupled to the structure.	0.5
METH	Method for advecting fluid mesh between solution time steps.	3
PC	Tensile cutoff pressure for fluid.	14.7 psi
Instantaneous Gravity	Method of applying gravity.	Gravity ramped over 0.01 seconds prior to impact.
Rigid Model	Treating the hemisphere model as rigid rather than flexible.	Flexible model.
61.3 lb Model	Weight of hemisphere.	48.0 lb
Divot	Adding a divot with a depth of 0.02 inches in way of the pressure transducer location.	No divot.

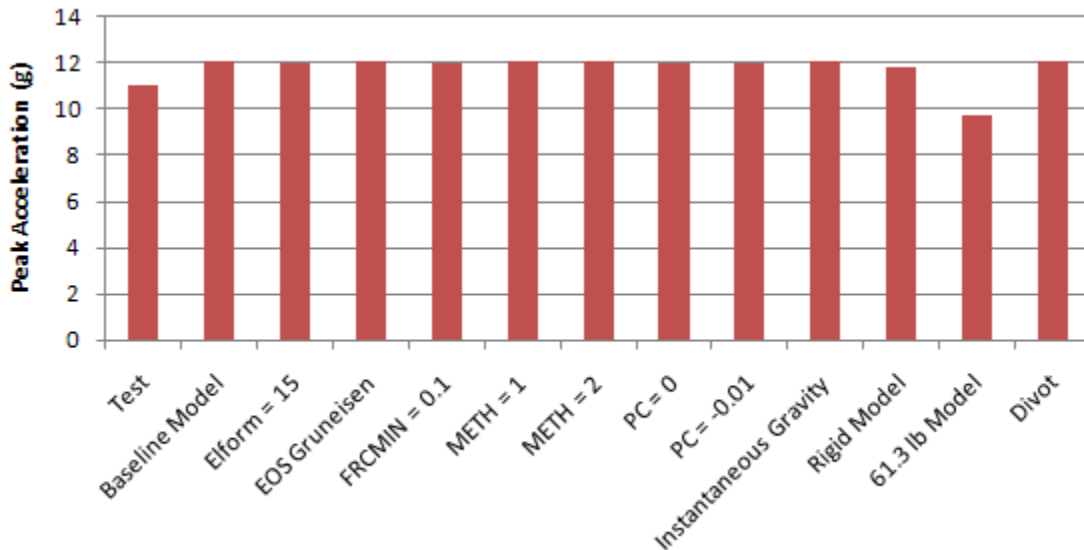


Figure 40. Peak Filtered Accelerations for Sensitivity Study Variants

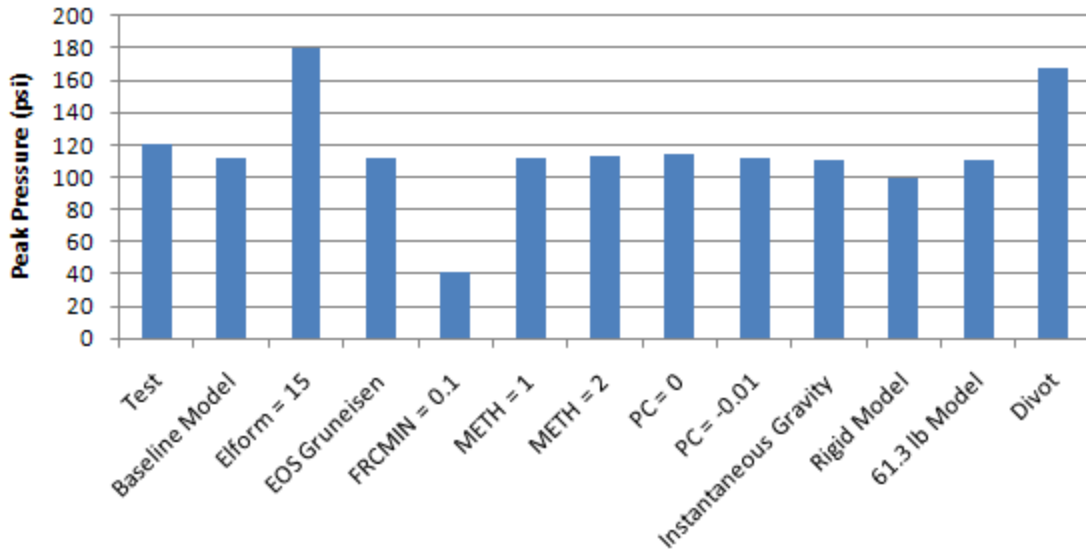


Figure 41. Peak Pressures for Sensitivity Study Variants

Regarding these parameters, the following should be noted.

- ELFORM=15 does not compute the stress correctly and should not be used according to the LS-DYNA developers at LSTC.
- The value of FRCMIN should be changed with caution as a low value can result in the fluid mesh moving before the impacting object arrives.
- METH=2 is described in the LS-DYNA Keyword User's Manual [2] as "second order accurate", whereas METH=1 and METH=3 (Baseline) are described as "first order accurate".
- PC=-14.7 is used to mimic the overpressure of the atmosphere. The result is that the water at the surface of the fluid mesh does not cavitate until a tensile pressure of 14.7 psi is reached.
- Initiating gravity instantaneously results in an oscillating pressure field in the fluid whereas ramping gravity results in a stable hydrostatic pressure field.
- The measured weight of the hemisphere was 48 lbs. The 61.3 lb weight was based on the basic geometry assuming that the bismuth was sold rather than machined away to accommodate instrumentation.

Increasing the weight of the hemisphere would be expected to reduce the peak deceleration. This is consistent with the simulation results. The reduced deceleration would result in a modestly higher velocity at the time that the pressure pulse reaches the transducer location, which would be expected to result in a higher pressure peak. The simulation showed negligible change in the peak pressure. The effect of the increased weight on the pressure history was so small that no clear effect was perceptible in the simulation.

The idea of adding a divot to the simulation model stemmed from the difficulty of obtaining a perfectly flush mounting for a pressure transducer in the test article. For the 2-D axisymmetric model, the

representation of a recessed transducer mounting as a divot was not exactly correct as the divot actually represented an axisymmetric groove; however, the effect was expected to be similar. The 0.02-inch divot resulted in a significant spike in the pressure as the water passed over it. This is illustrated in Figure 42 for a 5-foot drop of the 0.025-inch mesh with the 10 x Curve 10 coupling stiffness. This was consistent with findings from experiments with pressure transducers that showed that slightly recessing the pressure transducer resulted in a higher pressure reading.

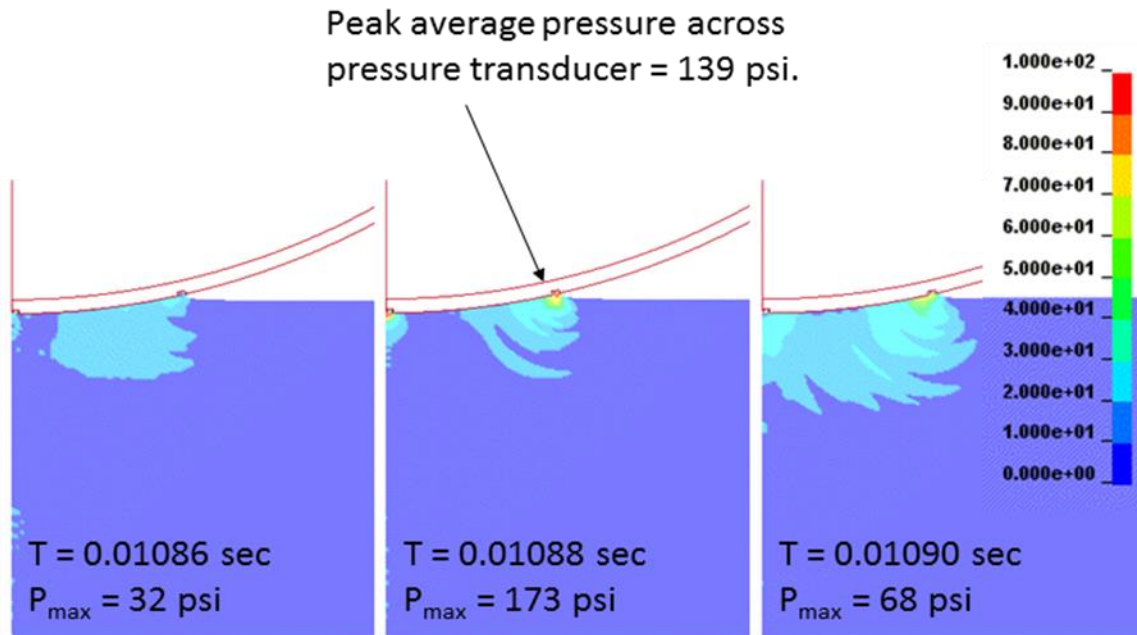


Figure 42. Pressure Pulse Caused by a 0.02-inch Divot

The conclusion from the results from the 2-D model was that the most important parameters for the study of test versus analysis correlation are mesh density and coupling stiffness. Other parameters either have little effect or lack any physical basis for making a change. As a consequence, mesh density and coupling stiffness were the focus of further studies performed with the three-dimensional model of the hemisphere.

5.3. 3-D LS-DYNA Results

A series of coupling stiffness variants for the baseline mesh (0.1-inch elements) were analyzed. In Figures 43 and 44, the acceleration histories for the 5-foot and 10-foot drops are compared to test data. For both drop heights, the simulation acceleration histories correlate well with the test data. The variant with the lowest coupling stiffness (0.1 x Curve 12) shows oscillatory behavior, which resulted from the hemisphere bouncing on the coupling surface.

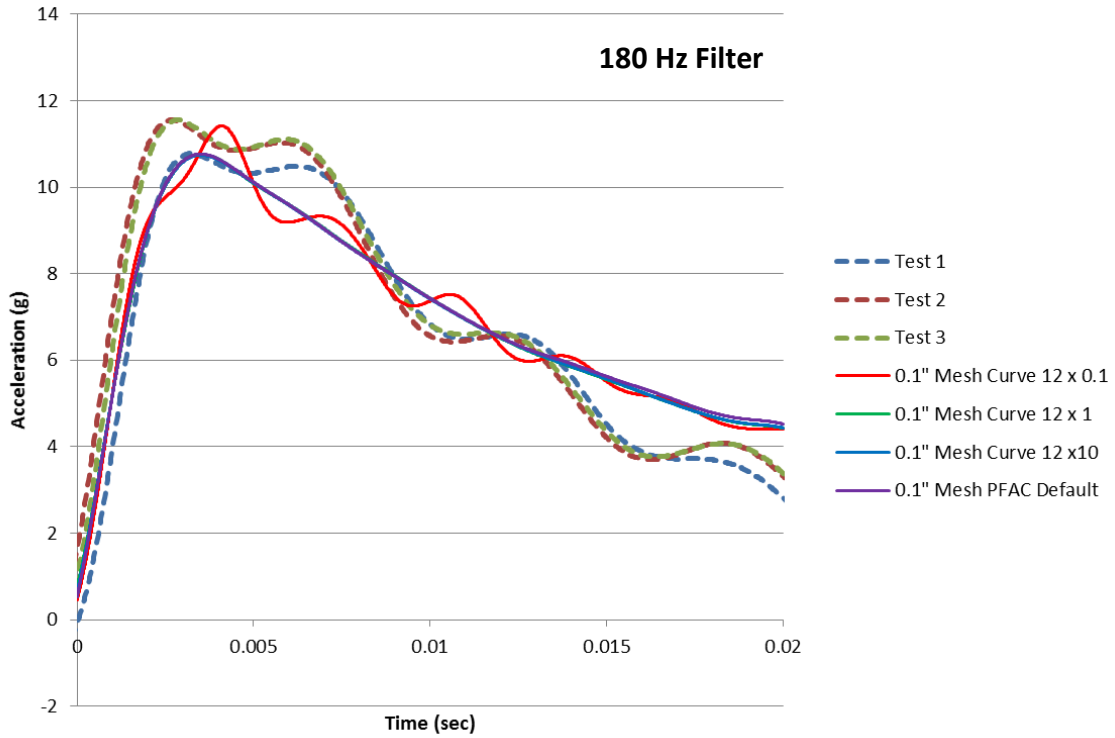


Figure 43. Acceleration History for 5-foot Drop Simulations

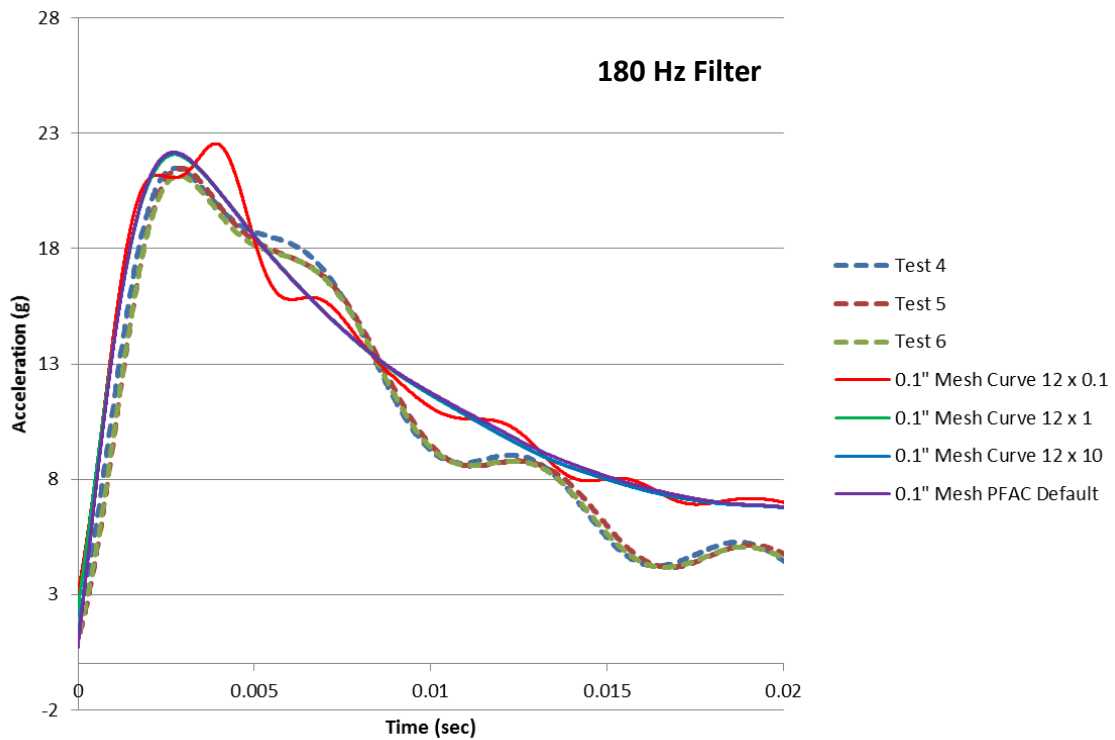


Figure 44. Acceleration History for 10-foot Drop Simulations

The pressure histories from the simulations are compared to test data in Figures 45 and 46. The simulation pressure histories show a strong sensitivity to coupling stiffness. The baseline coupling stiffness (Curve 12 x 1) shows the closest match to the peak pressures measured in the test; however, the shape of the curve from the simulation does not match the shape of the curves from the test.

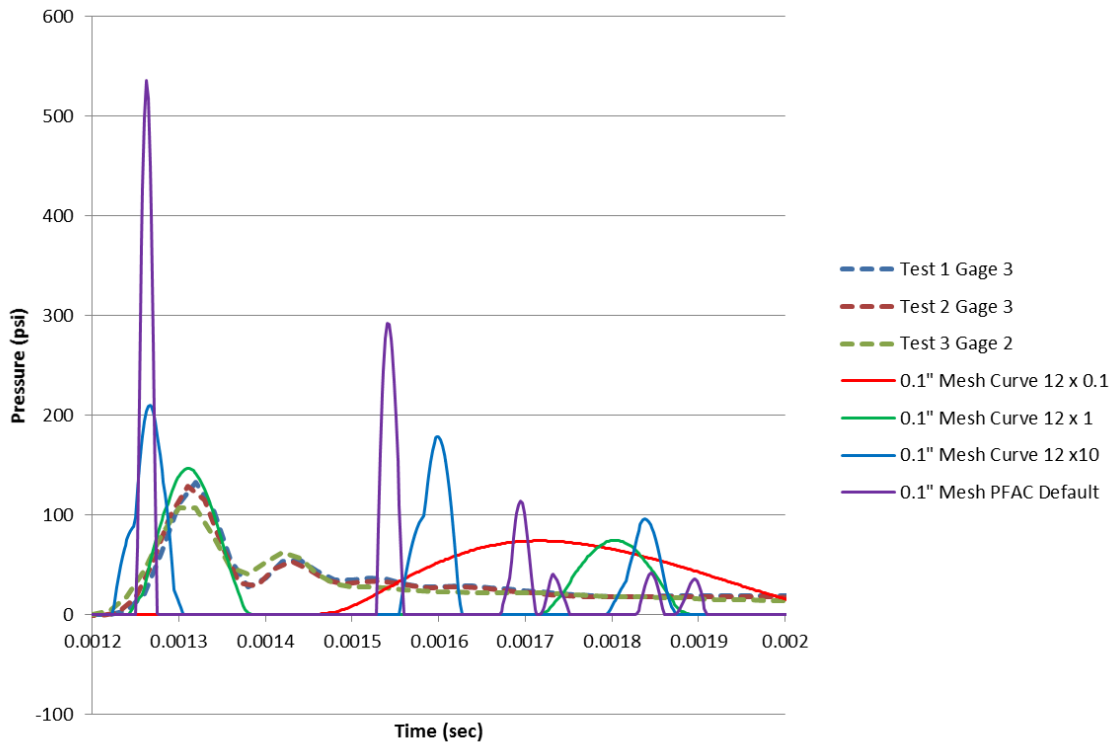


Figure 45. Pressure Histories for 5-foot Drop Simulations

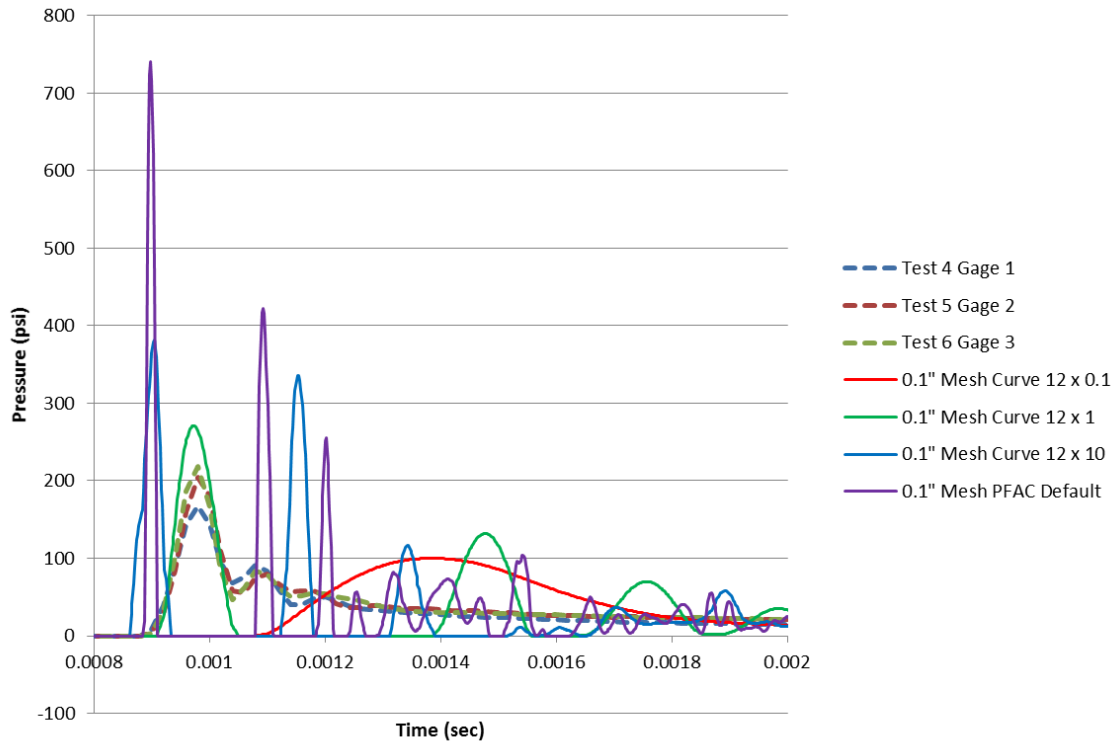


Figure 46. Pressure Histories for 10-foot Drop Simulations

For simulations of the 5-foot drops, the impulse during the first 0.01 seconds after impact varied between 0.052 psi-sec for the Curve 12 x 10 variant and 0.067 psi-sec for the Curve 12 x 1 variant. For the 5-foot drop test data, the range was 0.084 psi-sec to 0.116 psi-sec. For simulations of the 10-foot drops, the impulse varied between .098 for the Curve 12 x 10 variant and 0.100 for the PFAC Default variant. For the 10-foot drop test data, the range was 0.119 psi-sec to 0.122 psi-sec.

Figures 47 and 48 illustrate the distribution of the coupling pressure in the simulations of the 5-foot and 10-foot drops. The softest coupling stiffness (0.1 x Curve 12) produced a broad pressure patch without a well-defined “Coliseum Effect” ring of high pressure at its perimeter. The highest coupling stiffness (PFAC Default) produced a scattering of high pressure spikes rather than continuous rings of pressure.

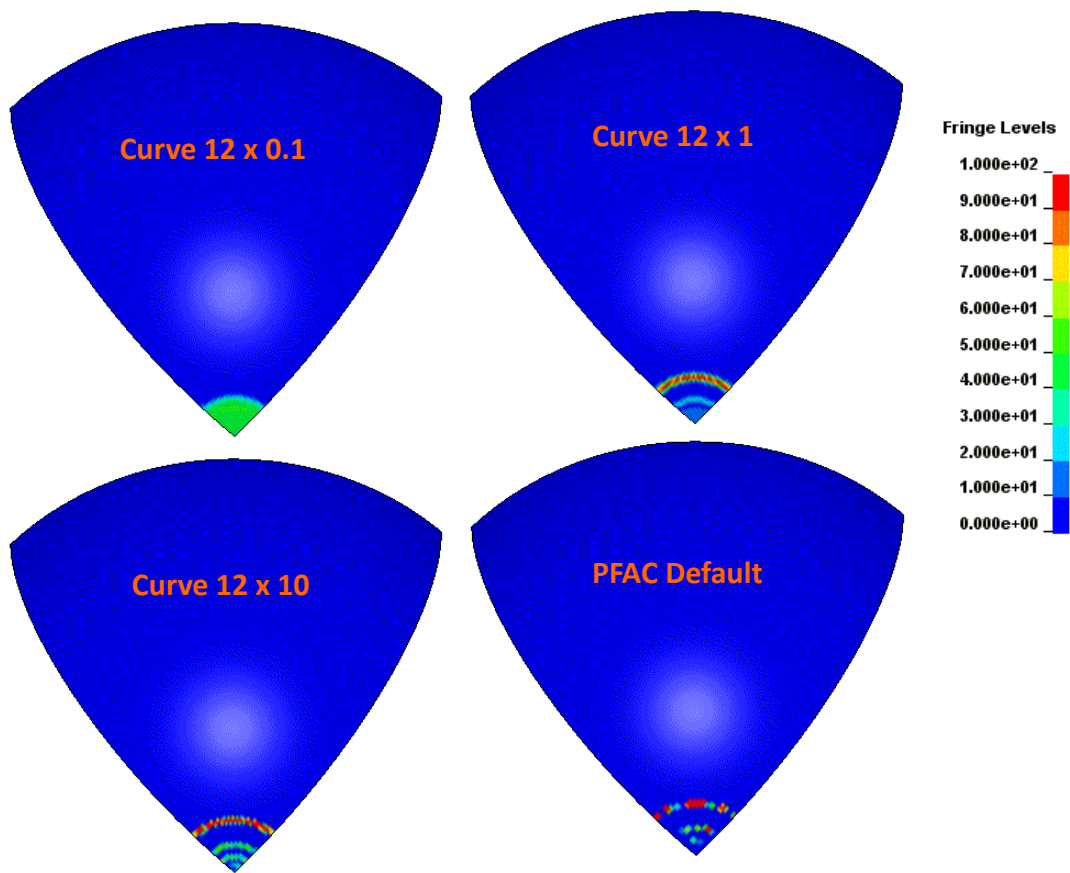


Figure 47. Pressure Distribution at 0.001 seconds after Impact for 5-foot Drop Simulations

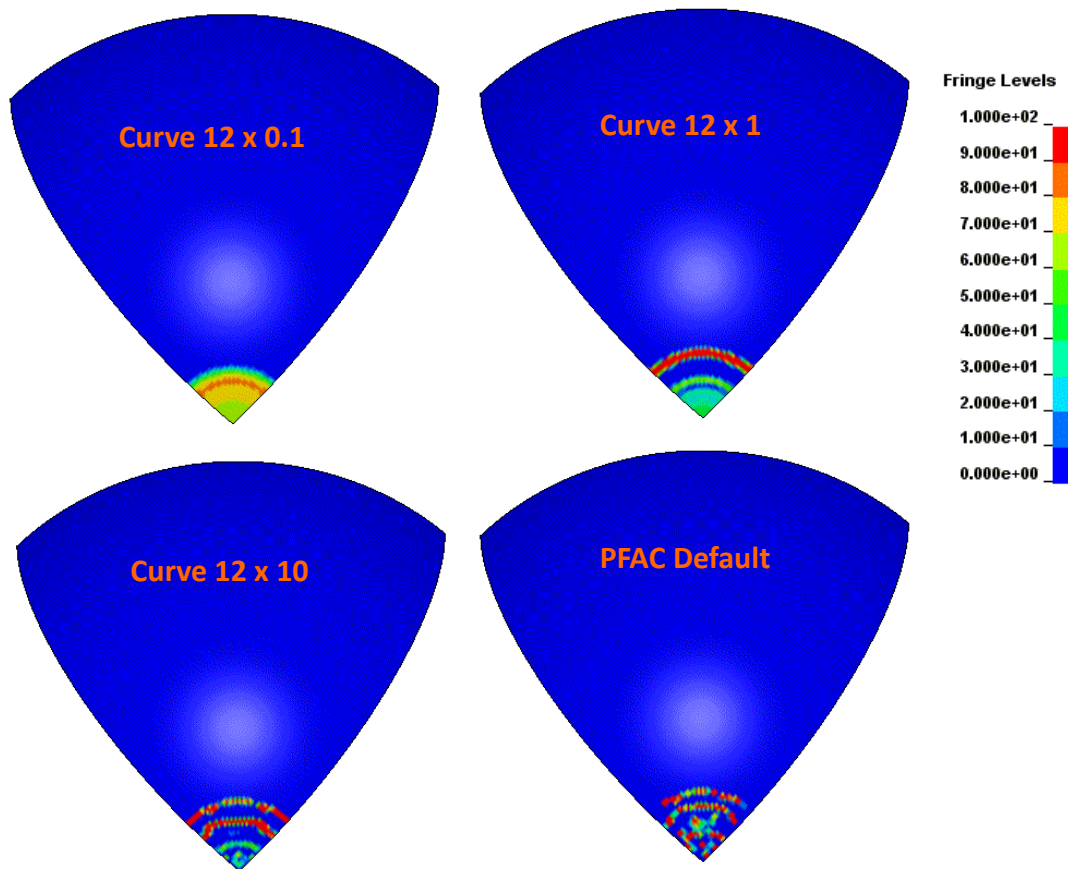


Figure 48. Pressure Distribution at 0.001 seconds after Impact for 10-foot Drop Simulations

Simulations were run for fluid mesh variants with element sizes of 0.05 inches and 0.025 inches. The element size of the hemisphere was 0.1 inches for all simulation variants. The 0.05-inch fluid mesh was created by subdividing the 0.1-inch elements of the baseline fluid mesh. The 0.025-inch fluid mesh was created by halving the dimensions of the 0.05-inch mesh. As a consequence, the 0.025-inch fluid mesh has just half the overall extent of the 0.1-inch and 0.05-inch fluid meshes. For the 0.025-inch fluid mesh, the hemisphere began to interact with the mesh boundary at approximately 0.002 seconds. This limited the 0.025-inch fluid mesh simulation to the very early time response.

For the 0.05-inch fluid mesh, the coupling stiffness was made twice as stiff as the Curve 12 baseline. For the 0.025-inch fluid mesh, coupling stiffness was made four times as stiff as the Curve 12 baseline. The increase in coupling stiffness for the finer meshes was motivated by the belief that the maximum allowable penetration distance should be a function of the fluid element size rather than an absolute dimension. Also, the number of fluid coupling points (NQUAD) was increased from 2 for the 0.1-inch baseline fluid mesh to 3 for the 0.05-inch fluid mesh and 6 for the 0.025-inch fluid mesh. This was necessary to avoid the smaller fluid elements slipping between the coupling points of the 0.1-inch elements of the hemisphere.

Acceleration histories for the 5-foot and 10-foot drops for the fluid mesh variants are compared to test data in Figures 49 and 50. The 0.025-inch fluid mesh is not included in the acceleration comparison because the hemisphere begins interacting with the fluid mesh boundary before the peak acceleration was reached. The results show that the refinement from a 0.1-inch mesh to a 0.05-inch mesh makes negligible difference in the acceleration histories.

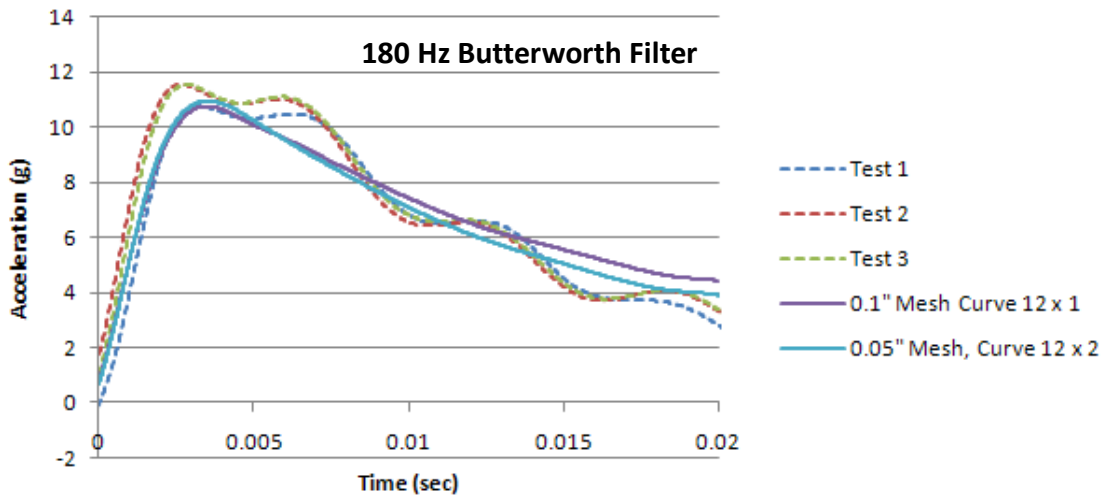


Figure 49. Acceleration Histories for Mesh Variants for 5-foot Simulations

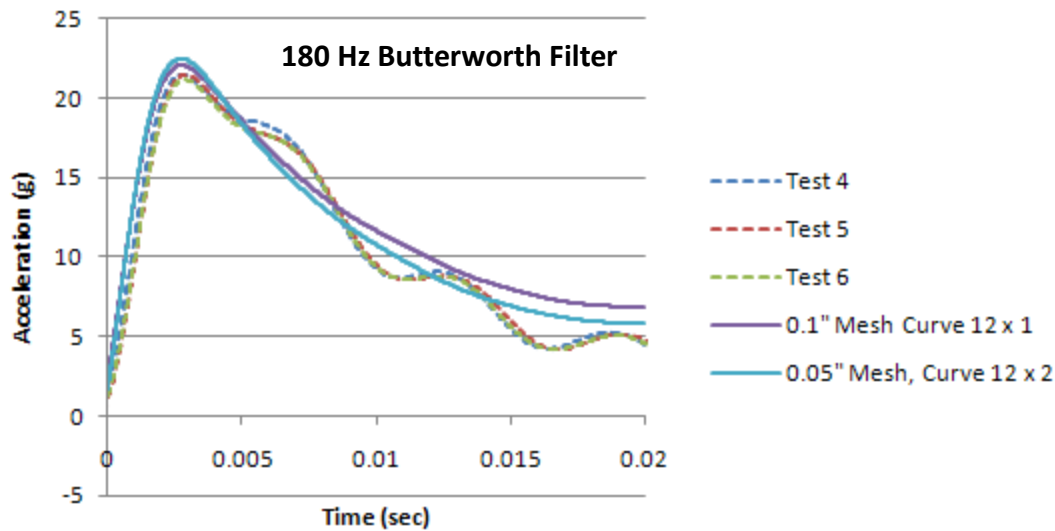


Figure 50. Acceleration Histories for Mesh Variants for 10-foot Simulations

Pressure histories for the fluid mesh variants are compared to test data in Figures 51 and 52. The pressure histories show that the baseline 0.1-inch mesh offers the best prediction for the peak pressure, but does not follow the pressure decay curves from the tests and has a second peak that is not physically reasonable. Refinement to a 0.05-inch mesh reduces the pressure peak below the value from the tests and results in a pressure history that oscillates about the pressure decay curves from the tests. Further

refinement to a 0.025-inch mesh further reduces the peak pressure and results in a pressure history that closely follows the pressure decay curves from the tests.

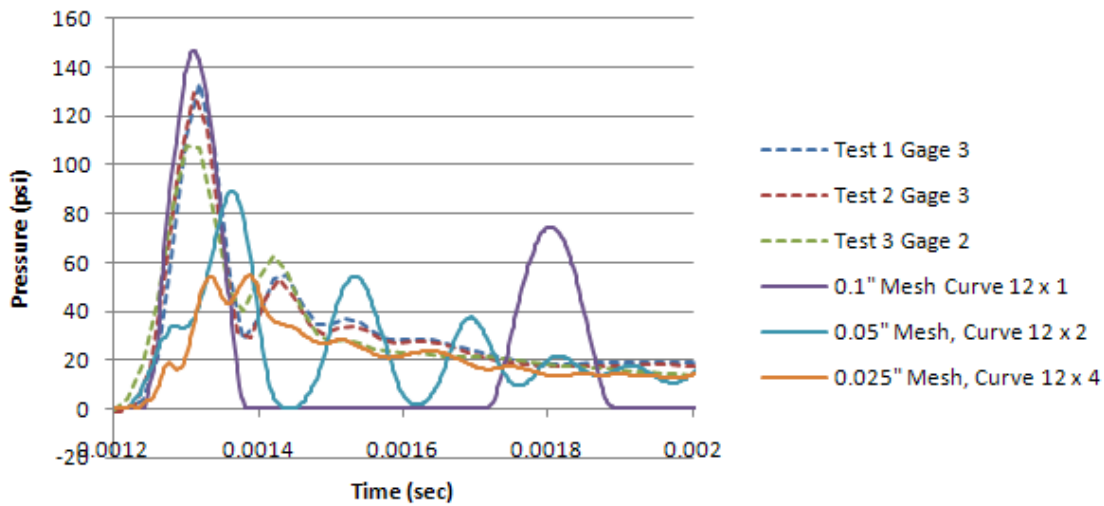


Figure 51. Pressure Histories for Mesh Variants for 5-foot Simulations

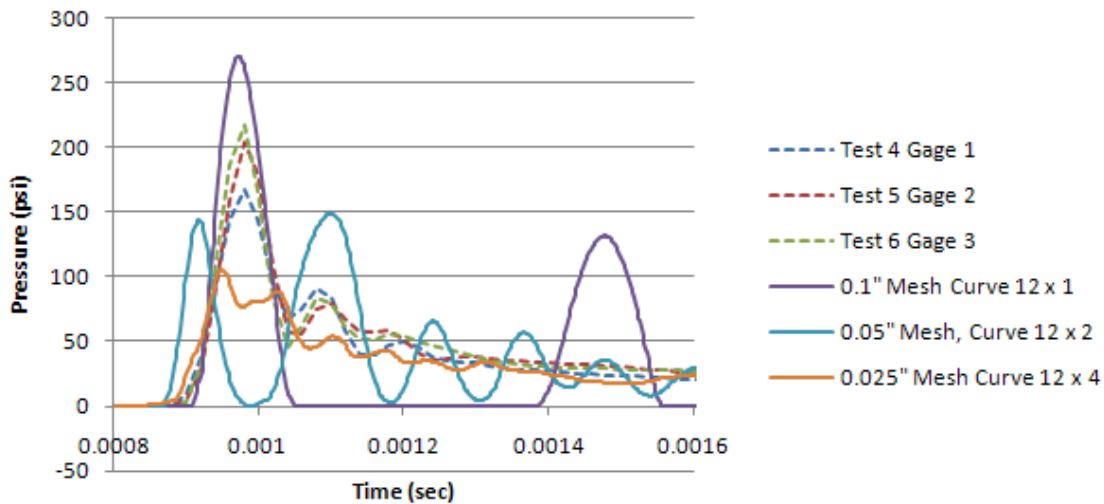


Figure 52. Pressure Histories for Mesh Variants for 10-foot Simulations

The simulation results for the 3-D model had peak filtered accelerations that were very similar to the test results. For the 5-foot drops, the simulations under-predicted the peak accelerations by less than 15%. For the 10-foot drops, the simulations modestly over-predicted the peak accelerations. The acceleration results support the use of a 15% allowance for design for loads that are proportional to the acceleration. The same cannot be concluded for the pressure histories. The peak pressures can be either over-predicted or under-predicted based on the mesh density and the coupling stiffness.

6. Establishing Simulation Parameters without Test Data

6.1. Width of Pressure Pulse

A series of tests were performed with additional pressure transducers mounted in the hemisphere. The time required for the pressure pulse to propagate from one transducer location to another provides an indication of the speed at which the pressure pulse travels. This can be used in conjunction with the observed time duration of the pressure pulse to estimate of the width of the pressure pulse. Figure 53 shows the arrangement of pressure transducers. Table 2 lists the coordinates of the pressure transducers.

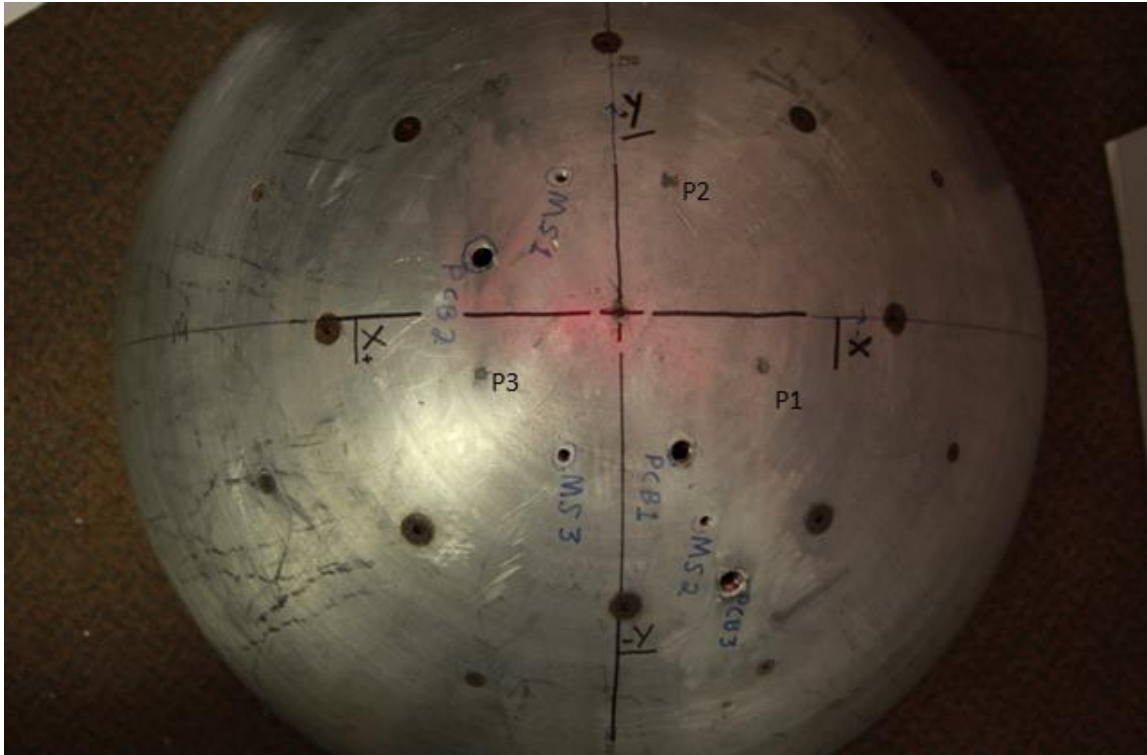


Figure 53. Pressure Transducer Arrangement

Table 2. Pressure Transducer Locations

Sensor ID	X (in)	Y (in)
MS1	0.8125	2.125
MS2	1.250	-3.1875
MS3	0.875	-2.0625
PCB1	-0.875	-2.0625
PCB2	3.0625	0.875
PCB3	-1.750	-4.1875

The histories for the pressure transducers for a 10-foot drop are shown in Figure 54. The peak pressure decreases, and the time duration increases, as the pressure pulse moves away from the apex. Table 3 provides an estimate of the width of the pressure pulse based on the time duration of the pulse and the

velocity of the pulse as determined from the arrival time at subsequent transducer locations. The calculation suggests a pulse width of approximately 0.2 inches, which is approximately 1/50th of the radius of the hemisphere.

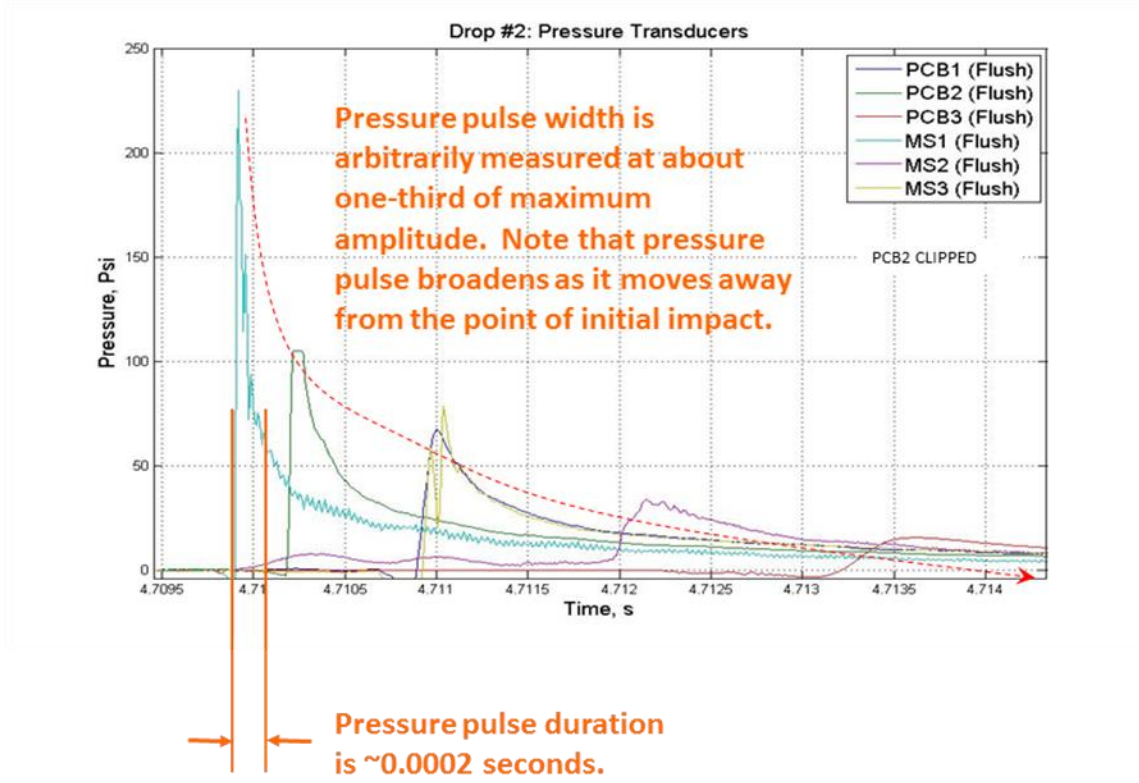


Figure 54. Pressure Histories for Multiple Pressure Transducers

Table 3. Pressure Pulse Width Estimate

Gage	Arrival Time (sec)	X (in)	Y (in)	Radius (in)	Velocity (in/sec)	Pulse Width (sec)	Pulse Width (in)
PCB1	4.711	-0.875	-2.0625	2.2404	986.17	0.0002	0.197
MS2	4.7122	-1.25	-3.1875	3.4238	857.41	0.0002	0.171
PCB3	4.7135	-1.75	-4.1875	4.5385	-	-	-

6.2. Establishing Mesh Density and Coupling Stiffness

The ability of the model to adequately simulate the pressure pulse is dependent on having a mesh density that adequately describes the shape of the pressure pulse. If it is assumed that a minimum of four elements are needed across the width of the pressure pulse, and it is estimated that the width of the pressure pulse is approximately 1/50th of the radius of curvature of the structure, then the fluid element size should be no larger than 1/200th of the radius of curvature. This leads to a fluid element size of 0.05 inches for the hemisphere. This is the element size for the middle mesh variant for the 2-D axisymmetric model. It is half the element size of the baseline 3-D quarter model.

The approach recommended by LSTC in the LS-DYNA Keyword User’s Manual [2] for defining the coupling stiffness curve is as follows.

“The curve consists of {0,0} as the first point and {maximum allowable penetration (MAP), estimated maximum coupling pressure (EMCP)} as a second point. MAP may be a small penetration with respect to the minimum ALE element width (maybe 10% or less). EMCP can be estimated from a maximum fluid pressure observed from a previous run when leakage first occurs. This curve may be scaled to vary the stiffness of the coupling spring. The approach is to gradually increase the coupling stiffness until leakage stops. The best coupling stiffness is one which provides just enough force to prevent leakage and not more”

LSTC subsequently amended this recommendation in e-mail and verbal communications. The amended recommendation is to base EMCP on the maximum pressure observed in a simulation with the PFAC default (PFAC = 0.1). There remains ambiguity as to whether this is the peak pressure seen anywhere in the model or at a presumed pressure transducer location and whether it should be the pressure seen in the fluid or at the fluid-structure interface. LS-DYNA does permit the specification of different fluid-structure coupling definitions (*CONSTRAINED_LAGRANGE_IN_SOLID) for different regions of the model; however, the coupling definition cannot be changed during the simulation.

For the hemisphere, the recommended mesh density and coupling stiffness are described in Table 4.

Table 4. Recommendations for Element Size and Coupling Stiffness

Parameter	Criteria	Value
Radius of Curvature, R	Known Dimension	10 in
Fluid Element Size, L	$L = R/200$	0.05 in
Maximum Allowable Penetration, MAP	$MAP = L/10$	0.005 in
Estimated Maximum Coupling Pressure, EMCP	From LS-DYNA simulation with PFAC = 0.1	100 psi

The maximum pressure is expected to be more than 10 psi but less than 1000 psi, so 100 psi was chosen as an order of magnitude estimate for EMCP. This resulted in a curve that is identical to Curve 10 (100 psi at 0.005 inch) used for the 2-D axisymmetric model. It is twice as stiff as Curve 12 (100 psi at 0.01 inch) used for the 3-D quarter model. It is recognized that even with these guidelines, the peak pressure is not likely to be predicted with a high degree of accuracy.

6.3. Evaluating Model Performance without Test Data

When test data is unavailable, the analyst must make judgments on the performance of the fluid-structure interaction to determine whether the coupling stiffness is too high or too low. Through the course of these and other simulations, several aspects of the model performance have been observed that provide indications regarding whether the behavior of a simulation is physically reasonable.

One way to assess the adequacy of the fluid-structure interaction is to observe the degree of penetration and leakage through the structure. The following distinction is made between penetration and leakage.

- Penetration is fluid that passes through the coupling interface but is still resisted by the coupling force.
- Leakage is fluid that escapes through the coupling interface and is not resisted by the coupling force.

Figure 55 illustrates the distinction between penetration and leakage.

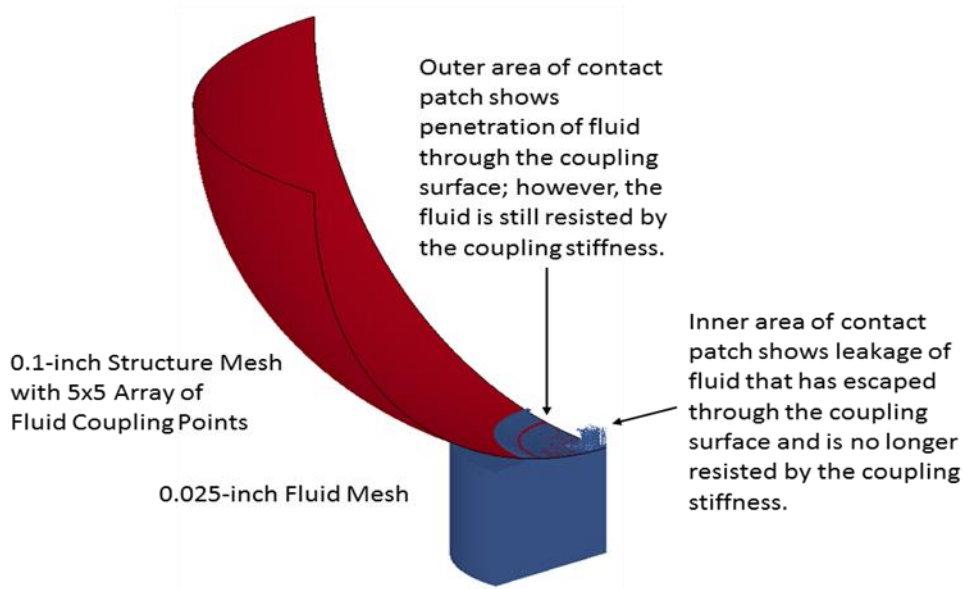


Figure 55. Description of Penetration and Leakage

Since LS-DYNA utilizes a penalty method in which springs are added to resist the passage of material through the coupling interface, some degree of penetration must always occur in order for there to be a coupling force. Penetration can be reduced by increasing the coupling stiffness (PFAC).

Leakage should not occur at a properly functioning fluid-structure interface. Leakage may occur if the relative mesh size is such that not every fluid element is resisted by coupling points on the structural elements. Leakage can be alleviated by increasing the density of the coupling points (NQUAD).

Two symptoms of an excessively soft coupling stiffness were observed. The first was a coupling pressure pattern that lacks a well-defined “Coliseum Effect” ring of high pressure at the outer perimeter of the contact patch. The second was low frequency oscillation of the acceleration history as a consequence of the oscillatory system created by the mass of the structure and the coupling stiffness. These symptoms are illustrated in Figure 56.

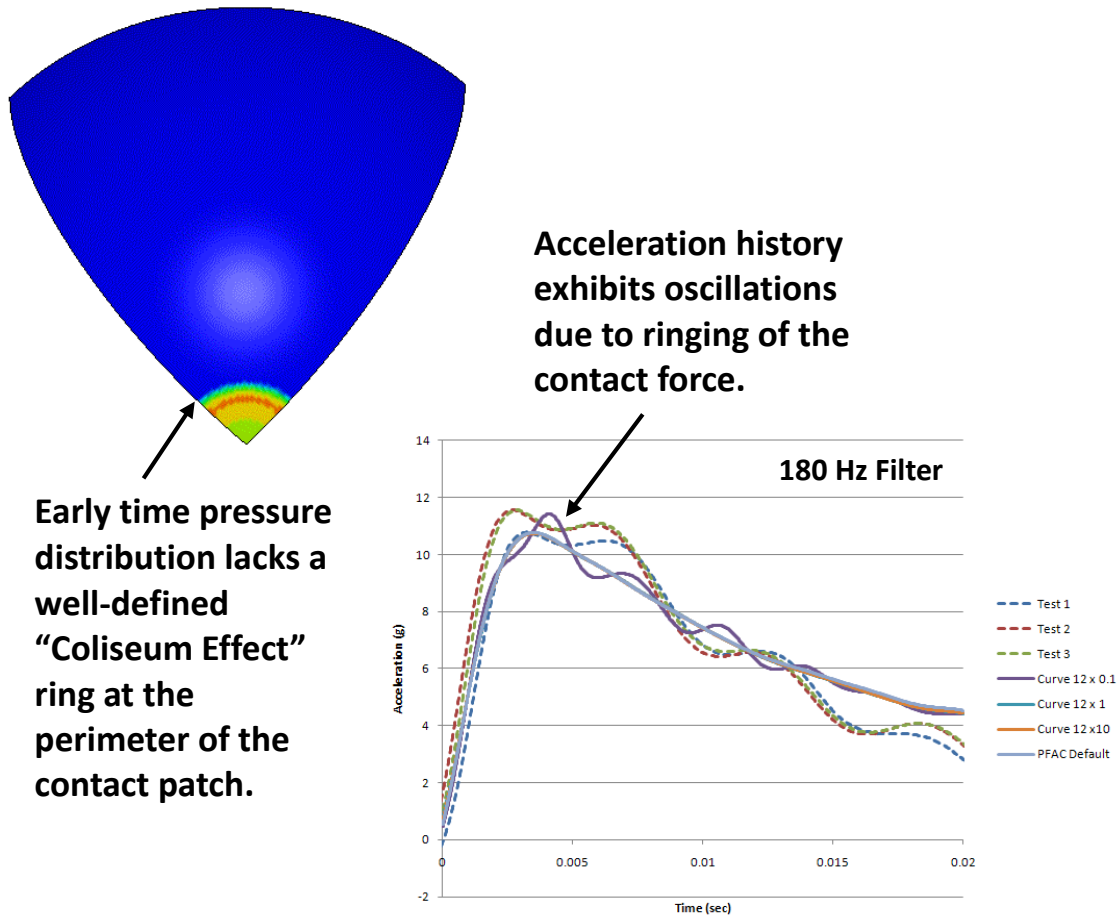


Figure 56. Symptoms of an Excessively Soft Coupling Stiffness

Two symptoms were also observed for an excessively stiff coupling stiffness. The first was an interface coupling pressure pattern that appears as a set of isolated point loads. The second was a pressure history that appears as a series of isolated high pressure spikes. These symptoms are illustrated in Figure 57.

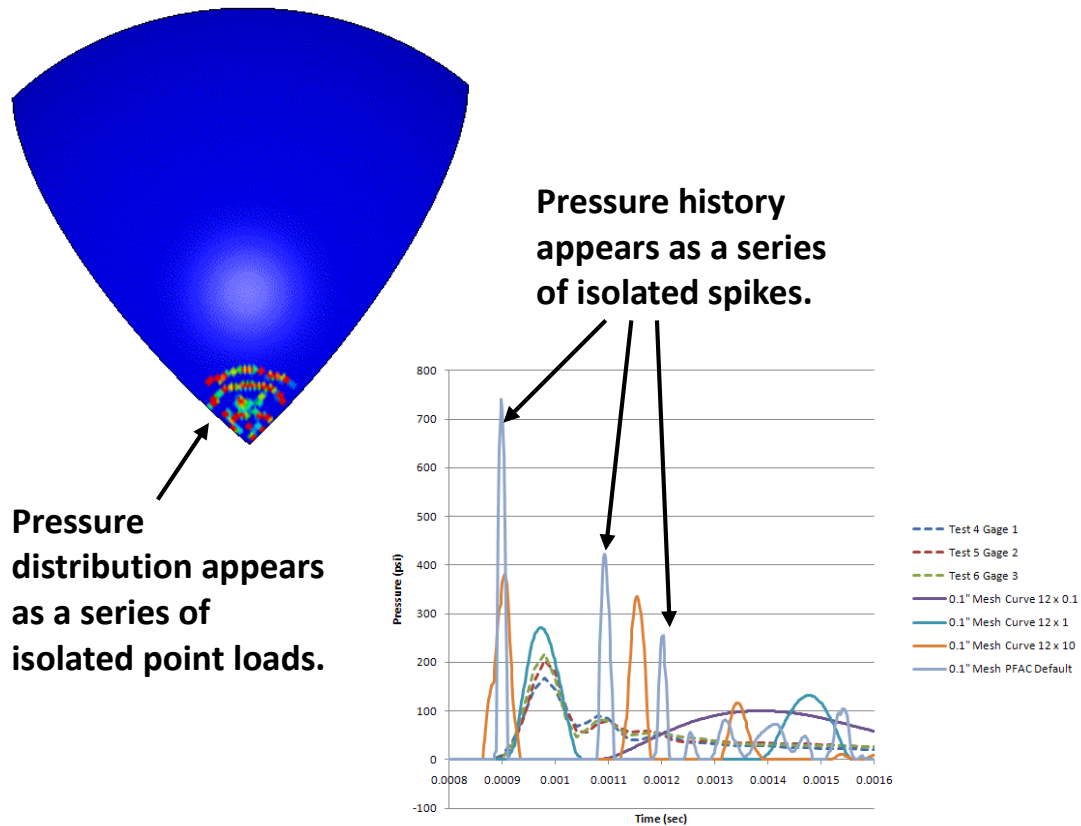


Figure 57. Symptoms of Excessively High Coupling Stiffness

These criteria can be used to evaluate coupling stiffnesses that are at the extremes. Unfortunately, this still leaves a broad range of coupling stiffnesses that are either too stiff or too soft but give results that are not obviously wrong.

7. Conclusions and Recommendations

The results for the hemisphere model demonstrate that LS-DYNA can accurately predict acceleration histories for a broad range of mesh densities and coupling stiffnesses. The prediction of pressure histories is a more difficult problem. LS-DYNA predictions of pressure histories improve as the fluid mesh is refined; however, the required mesh size for a real world problem may be impractical due to large model size requiring excessive disk space and unacceptably long run times.

The simulation results for the 3-D hemisphere model had peak filtered accelerations that were very similar to the test results. For the 10-foot drops, the simulations modestly over-predicted the peak accelerations. For the 5-foot drops, the simulations under-predicted the peak accelerations by less than 15%. This supports the use of a 15% allowance for design for loads that are proportional to the acceleration. The same cannot be concluded for the pressure histories. The peak pressures can be either over-predicted or under predicted based on the mesh density and the coupling stiffness.

In the absence of test data, the analyst must make a judgment regarding whether the fluid-structure coupling interface is performing adequately. The following guidelines are proposed.

1. The element size of the fluid mesh should be no larger than $1/200^{\text{th}}$ of the radius of curvature of the structure.
2. The coupling stiffness curve should be established based on the maximum expected coupling pressure at a penetration equal to $1/10^{\text{th}}$ the size of the fluid elements.

It is recognized that the above guidelines may result in an impractical model size with impractical run time and that the pressure histories are not likely to be realistic even if the guidelines are followed. As a consequence, the following guidelines for judging the adequacy of the performance of the coupling surface are offered.

1. The coupling stiffness is too soft if the peak coupling pressure is toward the middle of the contact patch rather than at the perimeter.
2. The coupling stiffness is too soft if the acceleration time history exhibits oscillations that can be related to the structure bouncing on the coupling surface.
3. The coupling stiffness is too stiff if the coupling pressure distribution appears as a checkerboard pattern of isolated pressure spikes.
4. The coupling stiffness is too stiff if the coupling pressure histories appear as a series of isolated spikes.

References

- [1] Hallquist, J.O., "LS-DYNA Theoretical Manual", LSTC Livermore, 1998.
- [2] "LS-DYNA Keyword User's Manual, Version 971," Livermore Software Technology Corporation, May 2007.
- [3] Cappelli, A.P. and Wilkinson, J.P.D., "Study of Apollo Water Impact, Final Report, Volume 2, Dynamic Response of Shells of Revolution during Vertical Impact into Water – No Interaction," NASA CR 92020, North American Aviation, Inc., Space Division, May 1967.

Appendix A: Two-Dimensional Axisymmetric Model

The following are the LS-DYNA cards that control the material properties, contact, and initial conditions for the axisymmetric model. These particular cards are for the 0.05-inch mesh for the 10-foot drop with the Curve 10 x 1 coupling stiffness. Node numbers and the number of set segments for pressure output differ depending on the mesh density.

```

*KEYWORD 800000000
$ IMPACT AT_0.01 SECONDS
$ RAMPED GRAVITY
$ ELFORM=14 FOR AIR AND WATER
$ VARIABLE D3PLOT TIME STEP
*TITLE
2-D Axisymmetric Model of 20" Hemisphere
*CONTROL_TERMINATION
$ ENDTIM ENDCYC DTMIN ENDENG ENDMAS
  0.0200      0.0      0.0      0.0
$*CONTROL_PARALLEL
$4
*CONTROL_HOURLASS
  1      0.1
*CONTROL_ENERGY
$# HGEN RWEN SLNTEN RYLEN
  2      2
*CONTROL_OUTPUT
$# NPOPT NEECHO NREFUP IACCOP OPIFS IPNINT IKEDIT IFLUSH
  1      3
$# IPRTF
  0
$
$*DATABASE_RBDOUT
$ 0.000020
*DATABASE_NODOUT
  0.000020
*DATABASE_HISTORY_NODE
$ id1 id2 id3 id4 id5 id6 id7 id8
  400020 400024 4001553 4001557 4001975
*DATABASE_BINARY_D3PLOT
$# dt lcdt beam npltc
  0.0000200 7778
*DEFINE_CURVE
  7778 0 1.0 1.0 0.0 0.0 0
      0.00000 0.002000
      0.00990 0.002000
      0.01000 0.000020
      0.01210 0.000020
      0.01212 0.002000
      0.02000 0.002000
*DATABASE_BINARY_D3THDT
  999.999
$
*SET_MULTI-MATERIAL_GROUP_LIST
$ 3=Vacuum 2=Soil
  123
  2
*ALE_MULTI-MATERIAL_GROUP
  2 1
  3 1
$
*SET_PART_LIST
  1
  2 3
*SET_PART_LIST
  11
  1 11 12 21 22
*CONTROL_ALE
$ DCT NADV METH AFAC BFAC CFAC DFAC EFAC
  3 1 3 -1.0
$ START END AAFAC VFACT PRIT EBC PREF NSIDBEC

```

```

$
*CONSTRAINED_LAGRANGE_IN_SOLID_EDGE
$#  slave  master  sstyp  mstyp  nquad  ctype  direc  mcoup
    11     1     0     0     3     4     2    -123
$#  start  end  pfac  fric  frcmin  norm  normtyp  damp
    0     0    -10     0     0     0     0     0
$#    cq    hmin  hmax  ileak  pleak  lcidpor  nvent  iblock
    0     0     0     0     0.1    0     0     0
$#  iboxid  ipenchk  intforc  ialesof  lagmul  pfacmm  thkf
    0     0     1     0     0     0     0

$
*DEFINE_CURVE
$  lcid  sidr  sfa  sfo
    10     0.000  1.0  1.00
    0.005  0.0  100.0

$
*SECTION_SHELL
$  SID  ELFORM  SHRF  NIP  PROPT  IRID  ICOMP  SETYP
    1    14  0.83333  NIP  PROPT  IRID  ICOMP  1
$  T1  T2  T3  T4  NLOC  MAREA  IDOF  EDGSET
    1.  1.  1.  1.

*SECTION_SHELL
$  SID  ELFORM  SHRF  NIP  PROPT  IRID  ICOMP  SETYP
    98   14  0.83333  NIP  PROPT  IRID  ICOMP  1
$  T1  T2  T3  T4  NLOC  MAREA  IDOF  EDGSET
    1.  1.  1.  1.

*SECTION_SHELL
$  SID  ELFORM  SHRF  NIP  PROPT  IRID  ICOMP  SETYP
    99   14  0.83333  NIP  PROPT  IRID  ICOMP  1
$  T1  T2  T3  T4  NLOC  MAREA  IDOF  EDGSET
    1.  1.  1.  1.

*SECTION_ALE2D
$  SID  ALEFORM  AET  ELFORM
    2    11     AET  14

*SECTION_ALE2D
$  SID  ALEFORM  AET  ELFORM
    3    11     AET  14

$
*PART
Vacuum
$  PID  SECID  MID  EOSID  HGID  GRAV  ADAPT  TMID
    2     3     3     0     3     0     0     0

$
*PART
Water
$  PID  SECID  MID  EOSID  HGID  GRAV  ADAPT  TMID
    3     2     2     2     2     0     0     0

$
*PART
Hemisphere
$  PID  SECID  MID  EOSID  HGID  GRAV  ADAPT  TMID
    1     1     1     0     1     0     0     0
SET SEGMENT 11 ELEMENT
    11     1     1     0     1     0
SET SEGMENT 12 ELEMENT
    12     1     1     0     1     0
SET SEGMENT 21 ELEMENT
    21     1     1     0     1     0
SET SEGMENT 22 ELEMENT
    22     1     1     0     1     0
Bismuth
    98     98     98     0     1     0
Cover
    99     99     99     0     1     0

$
$
*MAT_VACUUM
$  mid  rho
    3  1.116E-11

*MAT_NULL
$  mid  ro  pc  mu  terod  cerod  ym  pr
    2  9.3365e-5  -14.7  1.6300E-7  0.0000000  0.0000000

*MAT_ELASTIC
    1  0.000253  10.2E6  0.33  0

```

```

*MAT_ELASTIC
 98 0.0006279      4.6E6      0.33      0

*MAT_ELASTIC
 99 0.000253      10.2E6     0.33      0

$
*EOS_LINEAR_POLYNOMIAL
 2 0.0000000 3.11574e5 0.0000000 0.0000000 0.0000000 0.0000000
 0.0      1.0
$
*Hourglass
$  HGID      IHQ      QM
   3         1      1.E-6
   2         1      1.E-6
   1         1      0.1
*SET_NODE_LIST_GENERATE
$  sid
   111
$  blbeg      b1end
 4000001     4100000
*INITIAL_VELOCITY
$  nsid
   111
$  vx      vy      vz      vxr      vyr      vzr
   0.     -302.48     0.      0.0      0.0      0.0
*LOAD_BODY_Y
 1      386.1
*DEFINE_CURVE
 1         0      1.0      1.0      0.0      0.0      0
         0.0      0.0      0.0
         0.01     1.0
         100.0    1.0
$
*INCLUDE
2d_hemisphere_water_block_rev4_0p050.k
*DEFINE_TRANSFORMATION
 100
$  a1      a2      a3      a4      a5      a6      a7
TRANSL     0.0     13.04     0.
$
*INCLUDE_TRANSFORM
2d_20inch_hemisphere_0p050.k
$  idnoff  ideoff  idpoff  idmoff  idsoff  idfoff  iddoff
 4000000  4000000
$  idroff
$  fctmas  fcttim  fctltn  fcttem  incout1
         1
$  tranid
 100
$
*END

```

Appendix B: Three-Dimensional Quarter Model

The following are the LS-DYNA cards that control the material properties, contact, and initial conditions for the three-dimensional quarter model. These particular cards are for the 0.1-inch mesh for the 10-foot drop with the Curve 12 x 1 coupling stiffness. For the 0.05-inch mesh, the number of fluid-structure coupling points, NQUAD, is increased to 3. For the 0.025-inch mesh, NQUAD is increased to 6.

```

*KEYWORD 800000000
*TITLE
3D QUARTER MODEL OF HEMISPHERE
*CONTROL_TERMINATION
$  ENDTIM  ENDCYC  DTMIN  ENDENG  ENDMAS
   0.02    0.0    0.0    0.0    0.0
*CONTROL_HOURLASS
   1      0.1
*CONTROL_ENERGY
$#  HGEN    RWEN    SLNTEN    RYLEN
   2      2
*CONTROL_OUTPUT
$#  NPOPT  NEECHO  NREFUP  IACCOP  OPIFS  IPNINT  IKEDIT  IFLUSH
   1      3
$#  IPRTF
   0
$
*DATABASE_GLSTAT
0.000020
*DATABASE_MATSUM
0.000020
*DATABASE_RBDOUT
0.000020
*DATABASE_BINARY_D3PLOT
$#  dt      lcdt    beam    npltc
   0.0002
*DATABASE_BINARY_FSIFOR
$  dt
$ 0.0000200    7778
   0.0002
*DATABASE_BINARY_D3THDT
999.999
$
*SET_PART_LIST
   1
   2      3      22      23
*SET_PART_LIST
222
   2      22
*SET_PART_LIST
323
   3      23
*ALE_MULTI-MATERIAL_GROUP
$  sid    idtype
   222    0
   323    0
*SET_MULTI-MATERAIL_GROUP_LIST
123
   2
*CONTROL_ALE
$#  dct      nadv      meth      afac      bfac      cfac      dfac      efac
   2      1      2      -1.0
$#  start    end      aafac      vfact      prit      ebc      pref      nsidebc
      14.7
$
*CONSTRAINED_LAGRANGE_IN_SOLID
$#  slave  master  sstyp  mstyp  nquad  ctype  direc  mcoup
   1      1      1      0      2      4      2      -123
$#  start  end      pfac   fric   frcmin  norm  normtyp  damp
   0      0     -12    0     0      0     0      0
$#  cq     hmin    hmax   ileak  pleak  lcidpor  nvent  iblock
   0      0     0     0     0.1   0.1     0
$#  iboxid ipenchk intforc ialesof lagmul  pfacmm  thkf

```

```

$          0          0          1          0          0
*DEFINE_CURVE
$      lcid      sidr      sfa      sfo
          12          0.000          1.0          1.00
          0.010          100.0
$
*SECTION_SHELL
$      sid      elform      shrf      nip      propt      irid      icomp      setyp
          1          1      0.8333333
$      t1      t2      t3      t4      nloc      marea      idof      edgset
          0.1875      0.1875      0.1875      0.1875
*SECTION_SOLID
$      SID      ELFORM      AET
          2          11
*SECTION_SOLID
$      SID      ELFORM      AET
          3          11
*SECTION_SOLID
$      SID      ELFORM      AET
          22         11          4
*SECTION_SOLID
$      SID      ELFORM      AET
          23         11          4
$
*PART
Hemisphere
$      PID      SECID      MID      EOSID      HGID      GRAV      ADAPT      TMID
          1          1          1
$
*PART
Vacuum
$      PID      SECID      MID      EOSID      HGID      GRAV      ADAPT      TMID
          2          2          2          2          2          0
$
*PART
Water
$      PID      SECID      MID      EOSID      HGID      GRAV      ADAPT      TMID
          3          3          3          3          3          0
$
*PART
Vacuum
$      PID      SECID      MID      EOSID      HGID      GRAV      ADAPT      TMID
          22         22          2          2          2          0
$
*PART
Water
$      PID      SECID      MID      EOSID      HGID      GRAV      ADAPT      TMID
          23         23          3          3          3          0
$
*MAT_NULL
$      mid      rho      pc      mu      terod      cerod      ym      pr
          2      1.127E-7      0.0
*MAT_NULL
$      mid      rho      pc      mu      terod      cerod      ym      pr
          3      9.3365e-5      0.0      1.6300E-7      0.0000000      0.0000000
*MAT_RIGID
$      mid      ro      e      pr
          1      0.001075      1e+07      0.3
$      cmo      con1      con2
          1          5          7
$      a1      a2      a3      v1      v2      v3
$
*$EOS_IDEAL_GAS
$$      eosid      cv      cp      c1      c2      t0      v0
$          2      6.179E5      8.651E5      0.0      0.0      527.67      1.0
*$EOS_LINEAR_POLYNOMIAL
$      eosid      c0      c1      c2      c3      c4      c5      c6
          2          0.0      0.0      0.0      0.0      0.4      0.4      0.0
$      e0      v0
          36.74      0.0
$
*$EOS_LINEAR_POLYNOMIAL

```

```

$ eosid      c0      c1      c2      c3      c4      c5      c6
$           3      14.7  3.11574e5  0.0000000  0.0000000  0.0000000  0.0000000
$           e0      v0
$           0.0      0.0

$
*Hourglass
$   HGID      IHQ      QM
$           2      1      1.E-6
$           3      1      1.E-6

*SET_NODE_LIST_GENERATE
$   sid
$   111
$   blbeg      blend
$   4000001      4900000

*INITIAL_VELOCITY
$   nsid
$   111
$   vx      vy      vz      vxr      vyr      vzr
$   304.41      0.      0.
*LOAD_BODY_X
$   1      -386.1
*DEFINE_CURVE
$   1      0      1.0      1.0      0.0      0.0      0
$           0.0
$           100.0      1.0

*SET_PART_LIST
$   sid
$   781
$   pid1      pid2
$   2      3
*INITIAL_HYDROSTATIC_ALE
$   SID      SIDTYPE      VECID      GRAVITY      PBASE
$   781      0      789      386.1      14.7
$   NID      MMGBELOW
$   103067      1
$   44      2

*SET_PART_LIST
$   sid
$   782
$   pid1      pid2
$   22      23
*ALE_AMBIENT_HYDROSTATIC
$   SID      SIDTYPE      VECID      GRAVITY      PBASE
$   782      0      789      386.1      14.7
$   NID      MMGBELOW
$   103067      1
$   44      2

*DEFINE_VECTOR
$   vid      xt      yt      zt      xh      yh      zh      cid
$   789      0.      0.      0.      1.      0.      0.

$
*INCLUDE
water_air_quarter_0p1.k
*DEFINE_TRANSFORMATION
100
$           a1      a2      a3      a4      a5      a6      a7
TRANSL      -10.01      0.0      0.0
$
*INCLUDE_TRANSFORM
hemisphere_mesh_rev0.k
$   idnoff      ideoff      idpoff      idmoff      idsoff      idfoff      iddoff
$   4000000      4000000
$   idroff

$   fctmas      fcttim      fctltn      fcttem      incout1
$           1
$   tranid
$   100
$
*END

```

REPORT DOCUMENTATION PAGE

*Form Approved
OMB No. 0704-0188*

The public reporting burden for this collection of information is estimated to average 1 hour per response, including the time for reviewing instructions, searching existing data sources, gathering and maintaining the data needed, and completing and reviewing the collection of information. Send comments regarding this burden estimate or any other aspect of this collection of information, including suggestions for reducing this burden, to Department of Defense, Washington Headquarters Services, Directorate for Information Operations and Reports (0704-0188), 1215 Jefferson Davis Highway, Suite 1204, Arlington, VA 22202-4302. Respondents should be aware that notwithstanding any other provision of law, no person shall be subject to any penalty for failing to comply with a collection of information if it does not display a currently valid OMB control number.
PLEASE DO NOT RETURN YOUR FORM TO THE ABOVE ADDRESS.

1. REPORT DATE (DD-MM-YYYY) 01-01 - 2015		2. REPORT TYPE Contractor Report		3. DATES COVERED (From - To) 10/01/2013 - 09/30/2014	
4. TITLE AND SUBTITLE Elemental Water Impact Test: Phase 1 20-inch Hemisphere				5a. CONTRACT NUMBER NNL12AA09C	
				5b. GRANT NUMBER	
				5c. PROGRAM ELEMENT NUMBER	
6. AUTHOR(S) Vassilakos, Gregory J.				5d. PROJECT NUMBER	
				5e. TASK NUMBER	
				5f. WORK UNIT NUMBER 747797.06.13.06.32.04.03	
7. PERFORMING ORGANIZATION NAME(S) AND ADDRESS(ES) NASA Langley Research Center Hampton, Virginia 23681				8. PERFORMING ORGANIZATION REPORT NUMBER	
9. SPONSORING/MONITORING AGENCY NAME(S) AND ADDRESS(ES) National Aeronautics and Space Administration Washington, DC 20546-0001				10. SPONSOR/MONITOR'S ACRONYM(S) NASA	
				11. SPONSOR/MONITOR'S REPORT NUMBER(S) NASA/CR-2015-218679	
12. DISTRIBUTION/AVAILABILITY STATEMENT Unclassified - Unlimited Subject Category 31 Availability: NASA STI Program (757) 864-9658					
13. SUPPLEMENTARY NOTES Langley Technical Monitor: Robin C. Hardy					
14. ABSTRACT Spacecraft are being designed based on LS-DYNA simulations of water landing impacts. The Elemental Water Impact Test (EWIT) series was undertaken to assess the accuracy of LS-DYNA water impact simulations. Phase 1 of the EWIT series featured water impact tests of a 20-inch spherical hemisphere dropped from heights of 5 feet and 10 feet. The hemisphere was outfitted with an accelerometer and three pressure gages. The focus of this report is the correlation of analytical models against test data.					
15. SUBJECT TERMS Correlation; Coupling stiffness; Element size; Hemisphere; Impacts; LS-DYNA; Landing; Simulations; Water					
16. SECURITY CLASSIFICATION OF:			17. LIMITATION OF ABSTRACT	18. NUMBER OF PAGES	19a. NAME OF RESPONSIBLE PERSON
a. REPORT	b. ABSTRACT	c. THIS PAGE			STI Help Desk (email: help@sti.nasa.gov)
U	U	U	UU	60	19b. TELEPHONE NUMBER (Include area code) (757) 864-9658